



PUBLISHED FOR SISSA BY SPRINGER

RECEIVED: January 10, 2012

ACCEPTED: February 8, 2012

PUBLISHED: February 20, 2012

Unbalanced holographic superconductors and spintronics

Francesco Bigazzi,^{a,b} Aldo L. Cotrone,^c Daniele Musso,^c Natalia Pinzani Fokeeva^{a,d,e}
and Domenico Seminara^{a,d}

^a*Dipartimento di Fisica e Astronomia, Università di Firenze,
Via G. Sansone 1, I-50019 Sesto Fiorentino, Firenze, Italy*

^b*INFN — Sezione di Pisa,
Largo B. Pontecorvo, 3, I-56127 Pisa, Italy*

^c*Dipartimento di Fisica, Università di Torino and INFN — Sezione di Torino,
Via P. Giuria 1, I-10125 Torino, Italy*

^d*INFN, Sezione di Firenze,
Via G. Sansone 1, I-50019 Sesto Fiorentino, Firenze, Italy*

^e*Institute for Theoretical Physics, University of Amsterdam,
Science Park 904, Postbus 94485, 1090 GL Amsterdam, The Netherlands*

E-mail: bigazzi@fi.infn.it, cotrone@to.infn.it, mussod@to.infn.it,
npinzani@fi.infn.it, seminara@fi.infn.it

ABSTRACT: We present a minimal holographic model for s-wave superconductivity with unbalanced Fermi mixtures, in $2 + 1$ dimensions at strong coupling. The breaking of a $U(1)_A$ “charge” symmetry is driven by a non-trivial profile for a charged scalar field in a charged asymptotically AdS_4 black hole. The chemical potential imbalance is implemented by turning on the temporal component of a $U(1)_B$ “spin” field under which the scalar field is uncharged. We study the phase diagram of the model and comment on the eventual (non) occurrence of LOFF-like inhomogeneous superconducting phases. Moreover, we study “charge” and “spin” transport, implementing a holographic realization (and a generalization thereof to superconducting setups) of Mott’s two-current model which provides the theoretical basis of modern spintronics. Finally we comment on possible string or M-theory embeddings of our model and its higher dimensional generalizations, within consistent Kaluza-Klein truncations and brane-anti brane setups.

KEYWORDS: AdS-CFT Correspondence, Holography and condensed matter physics (AdS/CMT)

ARXIV EPRINT: [1111.6601](https://arxiv.org/abs/1111.6601)

Contents

| | | |
|----------|--|-----------|
| 1 | Introduction and overview | 1 |
| 2 | Unbalanced superconductors | 5 |
| 2.1 | Unconventional superconductors | 6 |
| 3 | Unbalanced holographic superconductors | 6 |
| 3.1 | Ansatz and equations of motion | 8 |
| 3.2 | Boundary conditions | 9 |
| 4 | The normal phase | 10 |
| 4.1 | A criterion for instability | 12 |
| 5 | The superconducting phase | 13 |
| 5.1 | The condensate | 13 |
| 5.2 | Comments on the LOFF phase | 15 |
| 6 | Conductivities: holographic spintronics | 17 |
| 6.1 | The conductivity matrix | 17 |
| 6.2 | Holographic calculation of the conductivities | 19 |
| 6.3 | Conductivities in the normal phase | 21 |
| 6.4 | Conductivities in the superconducting phase | 25 |
| 7 | Comments on possible string embeddings | 30 |
| 7.1 | Adjoint fermion condensates | 30 |
| 7.2 | Fundamental fermion condensates | 31 |
| A | The Chandrasekhar-Clogston bound | 33 |
| B | Equations of motion in $d + 1$ bulk spacetime dimensions | 34 |
| B.1 | The normal phase | 35 |
| B.1.1 | Near horizon geometry | 35 |
| B.2 | Criterion for instability | 36 |

1 Introduction and overview

The occurrence of superconductive phases where two fermionic species contribute with unbalanced populations, or unbalanced chemical potentials, is an interesting possibility relevant both in condensed matter and in finite density QCD contexts (see [1] for a review). A chemical potential mismatch between the quarks is naturally implemented in high density

QCD setups due to mass and charge differences between the quark species. In metallic superconductors the imbalance can be induced by e.g. paramagnetic impurities, modeled by means of a Zeeman coupling of the spins of the conducting electrons with an effective external magnetic “exchange” field.

At weak coupling, unbalanced Fermi mixtures are expected to develop inhomogeneous superconducting phases, where the Cooper pairs have non-zero total momentum. This is the case of the Larkin-Ovchinnikov-Fulde-Ferrel (LOFF) phase [2, 3]. The latter can develop, at small values of the temperature, provided the chemical potential mismatch $\delta\mu$ is not too large (if the Fermi surfaces of the two species are too far apart, the system reverts to the normal non-superconducting phase) and not below a limiting value $\delta\mu = \delta\mu_1$ found by Chandrasekhar and Clogston [4, 5]. At this point, at zero temperature, the system experiences a first order phase transition between the standard superconducting and the LOFF phase. The experimental occurrence of such inhomogeneous phases is still unclear, and establishing their appearance in strongly-coupled unconventional systems from a theoretical point of view is a challenging problem.

The imbalance of spin populations in ferromagnetic materials is also a relevant ingredient of spintronics, the branch of electronics concerned with the study and applications of spin transport. Spintronics constitutes a very important research area, due to its technological outcomes, e.g. in computer hard disk devices. From the theoretical point of view, the research in this area is vast and quickly developing. See [6, 7] and references therein for interesting introductions to the subject.

The roots of spintronics are based on Mott’s “two-current model” [8, 9]. Mott’s model describes ferromagnetic materials at low temperature and in its simplest version it treats both charge and spin as conserved quantities, neglecting dissipative spin-flip interactions like spin-orbit terms. In the model, charge and spin currents flow in parallel and can be both induced either by turning on an electric field or a “spin motive force” [10–12]. The latter can be practically realized by a space gradient in the chemical potential imbalance, for example by means of a ferromagnetic-non ferromagnetic junction. The electric and spin motive forces can be described by means of two (“effective” in the case of the spin¹) U(1) gauge fields. This picture has been recently used in the system of degenerate free electrons subjected to impurity scattering in ferromagnetic conductors [14, 15]. It is an interesting problem to see how the two-current model can be realized in general setups (even superconducting ones) where a weakly coupled quasi-particle description cannot be employed.

With the aim of providing some toy-model-based insights on these issues, we have studied the simplest holographic realization of strongly coupled unbalanced s-wave superconductors in the grand-canonical ensemble at non-zero temperature.² Experimental evidence suggests that high T_c superconductors like certain cuprates are effectively layered. Moreover it is expected that they develop a quantum critical point (QCP) in their phase diagram [23, 24]. If the QCP displays conformal invariance, the physics at this point (and

¹In 3 + 1 dimensions, the U(1) spin symmetry is contained in the SU(2) spin group which is a good approximate symmetry at low energy and temperature, see e.g. [11–13].

²For an introduction to the literature on holographic studies of condensed matter systems see the reviews [16–22] and references therein.

within the so called critical region) is effectively described by a 2+1 dimensional conformal field theory at strong coupling (and at finite temperature and density). A related holographic description, within a simple bottom-up approach, is provided by a gravitational dual model in 3+1 dimensions with the following minimal ingredients. The breaking of a $U(1)_A$ “charge” symmetry characterizing superconductivity is driven, on the gravity side, by a non-trivial scalar field charged under a $U(1)_A$ Maxwell field in an asymptotically AdS_4 black hole background as in [25–27]. The chemical potential mismatch, which can also be interpreted as a chemical potential for a $U(1)_B$ “spin” symmetry (see also [13]), is accounted for in the gravity setup by turning on the temporal component of a Maxwell field $U(1)_B$ under which the scalar field is uncharged.³

The model depends on two parameters, namely the charge q of the scalar field and its mass m . For a particular choice of the latter (namely $m^2 = -2$ in units where the AdS radius is set to one), aimed at implementing a fermionic condensate of canonical dimension 2,⁴ we will show that the critical temperature below which a superconducting homogeneous phase develops decreases with the chemical potential mismatch, as it is expected in weakly coupled setups. However, the phase diagram arising from the holographic model shows many differences with respect to its weakly coupled counterparts. In particular there is no sign of a Chandrasekhar-Clogston bound at zero temperature and the superconducting-to-normal phase transition is always second order. This leads us to argue that a LOFF phase should not show up (we have checked that this is actually the case in the $q \gg 1$ limit). A different situation arises for different choices of the parameters which seem to allow for Chandrasekhar-Clogston-like bounds; we will not explore these choices in detail in this paper.

Using standard holographic techniques, we also study “charge” and “spin” transport in our model. Essentially we turn on an external electric field E^A as well as a “spin motive field” E^B and look at the correspondingly generated “charge” and “spin” currents J^A and J^B . The holographic model provides a quite natural realization of Mott’s two-current model.⁵ It also automatically provides a non-trivial conductivity matrix for the optical “charge”, “spin” and other conductivities (we study heat transport, too) at zero momentum, both in the superconducting and in the normal phase (which can be also seen as a holographic “forced” ferromagnetic phase [13]). The intertwining of spin and charge transport is mediated, holographically, by the interaction of the $U(1)_A$ and $U(1)_B$ Maxwell fields with the metric.⁶ This very general simple phenomenon, not related with particular

³Similarly, the holographic unbalanced p-wave setup of [28] contains $SU(2) \times U(1)_B$ gauge fields. An $U(1)_3 \subset SU(2)$ symmetry is broken by the condensation of e.g. a $U(1)_1 \subset SU(2)$ vector [29, 30] which is uncharged under $U(1)_B$.

⁴In 2+1 dimensions a weakly coupled Cooper pair has dimension 2.

⁵Different holographic models with two currents have been studied in the literature. Nevertheless, as far as we are aware of, the connection with the two-current model has not been explored so far.

⁶In our model this is the only way in which the two Maxwell fields can couple. In the dual field theory this implies that the corresponding currents are only coupled through “gluon-like” loops. This feature is model dependent: in other holographic setups, such as those with two overlapping “flavor” D-branes, the coupling can happen also more directly, e.g. by means of non linear terms in the brane action [28] or by $F_A \wedge F_B$ terms [31–33]. The coupling via the energy-momentum tensor operator is nevertheless generically present in these cases too.

assumptions in our model, suggests that analogous “spintronics” effects could occur in generic strongly coupled unbalanced models, for example in QCD at finite baryon and isospin density.

The phenomenological bottom-up holographic approach we adopt in this paper, aims at providing information on some universal properties of classes of strongly coupled field theories with the same (broken) symmetries and scales. Details on the dual microscopic theories could be provided by embedding our model in full-fledged string or M-theory constructions. We will consider embeddings within Kaluza-Klein reductions of eleven or ten dimensional supergravities as well as within brane-anti brane setups. In both cases we find indications that a consistent top-down realization of our model requires the addition of at least another non-trivial real scalar in the gravity action.

Organization of the paper and main results. This paper is organized as follows. In section 2 we provide a short review of the main features of unbalanced Fermi systems at weak coupling. In section 3 we present our gravity model and write down the corresponding equations of motion with appropriate ansätze for the gravity fields.

In section 4 we describe the $U(1)^2$ -charged Reissner-Nordstrom AdS solution corresponding to the normal non-superconducting phase, where the scalar field is zero. We discuss under which conditions this phase could remain stable at zero temperature under fluctuations of the scalar field envisaging the possibility of Chandrasekhar-Clogston-like bounds depending on the choices of the parameters (equation (4.14)).

In section 5 we present the results of the numerical analysis of the coupled differential equations when the scalar field has a non-trivial profile, i.e. in the superconducting phase. We thus describe the behavior of the condensate as a function of the temperature and the $(T_c, \delta\mu)$ phase diagram (figure 3), where T_c is found to be a never vanishing decreasing function of $\delta\mu/\mu$. We also briefly comment on the (non) occurrence of LOFF phases within our model focusing on the large charge $q \gg 1$ limit.

In section 6 we study the conductivity matrix at various values of $(T, \delta\mu)$ and the comparison with weakly coupled spintronics. Starting from our general formulas (6.20), (6.21), (6.23), we provide some precise relations among the various conductivities in the normal phase (formula (6.26)). Interestingly, in the superconducting phase we find that in our strongly coupled model the DC conductivity related to the “spin” is enhanced, analogously to the “electric” one. Moreover, the “pseudo-gap frequency” ω_{gap} in the superconducting phase is found to be non-linearly decreasing with $\delta\mu/\mu$; the same happens for ω_{gap}/T_c .

In section 7 we comment on possible string or M-theory embeddings, providing evidence that an extra uncharged scalar is probably needed for the purpose, even in the unbalanced normal phase. It would be relevant to understand the physical meaning of this field and the role it could play within possible holographic realizations of ferromagnetic phases with magnon order parameters. We end up with appendices containing some review material and technical details.

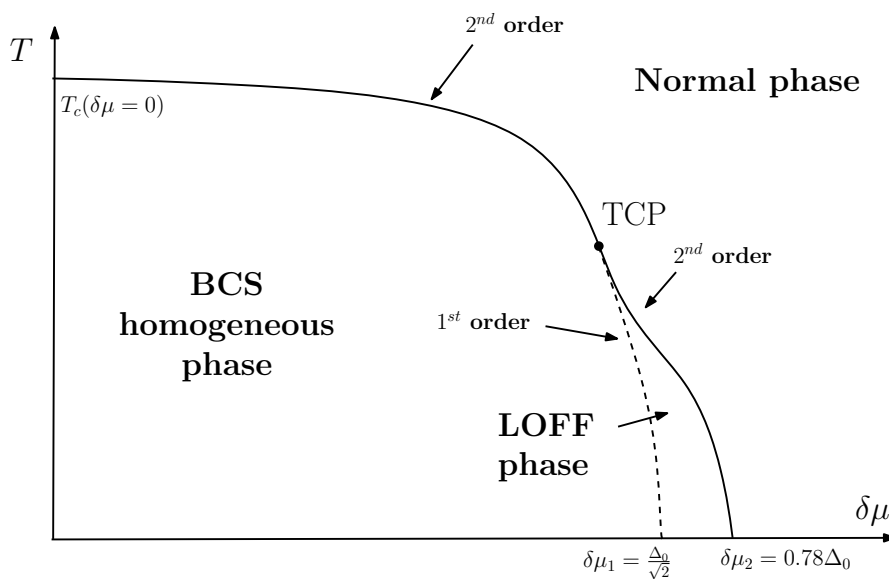


Figure 1. The $(T, \delta\mu)$ phase diagram for weakly coupled unbalanced superconductors.

2 Unbalanced superconductors

At weak coupling, where BCS theory can be applied, the physical properties of unbalanced superconductors as functions of the chemical potential mismatch $\delta\mu$ are well known. The $(T, \delta\mu)$ phase diagram is sketched in figure 1. At zero temperature, the imbalance produces a separation of the Fermi surfaces of the two fermionic species, so that their condensation into Cooper pairs is suppressed as $\delta\mu$ is increased. As it was shown by Chandrasekhar and Clogston [4, 5] (whose arguments we review in appendix A), the BCS superconducting phase becomes energetically unfavored whenever $\delta\mu$ exceeds a limiting value $\delta\mu_1 = \Delta_0/\sqrt{2}$, where Δ_0 is the BCS gap parameter at $T = \delta\mu = 0$. If no other phases would develop, at $\delta\mu = \delta\mu_1$ there would be a first order phase transition (with the gap jumping discontinuously from zero to Δ_0) from the normal to the superconducting BCS phase.

Increasing the temperature above zero, a line of first order phase transitions emerges from the point $(0, \delta\mu_1)$ in the $(T, \delta\mu)$ phase diagram. This line joins, at a critical point, with a line of second order transitions departing from $(T_c^0, 0)$ (at zero chemical potential mismatch, the phase transition is the standard BCS second order one). The critical temperature T_c below which the system is superconducting is a monotonically decreasing function of $\delta\mu$. But this is not the end of the story.

In 1964 Larkin and Ovchinnikov and independently Fulde and Ferrel [2, 3] showed that at $T = 0$, there is a window of values $\delta\mu_1 \leq \delta\mu \leq \delta\mu_2$ for which the energetically favored phase is an inhomogeneous superconducting (LOFF) phase, with Cooper pairs having a non-zero total momentum \vec{k} (see also [34] and [35] for reviews). The modulus $k = |\vec{k}|$ is fixed by free energy minimization with respect to k (this amounts to setting to zero the superconducting current) and it results to be proportional to $\delta\mu$. Its direction is chosen spontaneously. In general there could be crystalline phases where the fermionic condensate

is a combination of wave functions with differently directed \vec{k}_i vectors. The simplest (FF and LO) ansätze amount to just assume a plane wave or two-plane wave (sine or cosine) form for the condensate. In these cases, the LOFF-to-normal phase transition at zero temperature is second order and $\delta\mu_2$ is just slightly bigger than $\delta\mu_1$. In general, the width of the LOFF window in the phase diagram depends on the geometry of the crystal structure in momentum space.

At finite temperature, a line of second order phase transitions departs from the point $(0, \delta\mu_2)$ in the phase diagram, and ends up in the previously mentioned critical point which thus becomes a tricritical (TCP) one.

2.1 Unconventional superconductors

In metallic superconductors, the Zeeman coupling with an external magnetic field (which induces a chemical potential imbalance) is usually negligible with respect to the orbital coupling. The latter can be naturally reduced in layered setups, such as the high T_c cuprates or iron pnictides, by taking the external magnetic field directed along the layers. These unconventional compounds are thus promising candidates for looking at LOFF-like effects, though their non-BCS nature makes the previously mentioned theoretical analysis not reliable. The same remark holds for unbalanced superconducting quark matter [36–39] whenever perturbation theory cannot be applied (e.g. for the estimated quark densities in the core of neutron stars). In this case, one can get some insight by means of e.g. Nambu-Jona-Lasinio (NJL)-like effective field theories, while lattice computations suffering from the so-called sign problem are not well suited for finite density setups.

A promising setup where the LOFF effect can be experimentally investigated in various ranges of the “coupling”, is that of trapped cold Fermi gases (see [40] for a general review). The latter experience a crossover transition between a weakly coupled BCS and a strongly coupled BEC (Bose-Einstein Condensate) phase as some parameter is varied. Experiments [41] on cold atomic gases with unbalanced populations seem to suggest that a Phase Separation (PS) scenario [42] (with an homogeneous superfluid core and a normal surrounding shell) is realized instead of the LOFF one. However, a clear experimental evidence is still lacking, and the possibility of a LOFF phase emerging in some range of the coupling cannot be discarded. This issue has been theoretically investigated (in the mean field approximation) in e.g. [43] by means of NJL models with four-fermion interactions. It turns out that, at fixed total density, when the coupling is tuned from weak to strong (i.e. in the BEC phase) the one-plane-wave LOFF window shrinks to a point and then disappears as the coupling is increased. At strong coupling, the unique homogeneous superfluid phase exhibits one gapless mode and has a second order transition to the normal phase. We will see that most of these properties are reproduced by our holographic model.

3 Unbalanced holographic superconductors

As we have recalled in the Introduction, in the case of metallic superconductors, a chemical potential mismatch between spin “up” and “down” species can be induced by the Zeeman effect i.e. by the interaction term $\mathcal{H}_I = \bar{\Psi}\gamma^0 H_z \mu_B \sigma_3 \Psi$ in the Hamiltonian, between e.g.

paramagnetic impurities, modeled by an external magnetic field H_z and the spin of the fermions. Here μ_B is the Bohr magneton and $\sigma_3 = \text{diag}(1, -1)$. The effective chemical potential mismatch is given in this case by $\delta\mu = H_z\mu_B$. At low energy, the latter can be read as the temporal component of an effective $U(1)_B$ spin vector field B_μ (see also [13]). The two fermionic species have opposite “charges” with respect to $U(1)_B$, hence the up-down Cooper condensate (charged under an electromagnetic $U(1)_A$ vector field whose temporal component effectively provides the mean chemical potential μ) has zero total spin charge. This simple picture lies at the basis of our effective holographic model and can be applied to more general unbalanced setups (e.g. to QCD-like ones).

The simplest gravity model in 3+1 dimensions aiming at implementing holographically the main features of the quantum critical region of s-wave unbalanced unconventional superconductors in 2+1 dimensions is thus described by the following action (see appendix B for a generalization of this setting to any $d > 2$)

$$S = \frac{1}{2\kappa_4^2} \int dx^4 \sqrt{-g} \left[\mathcal{R} + \frac{6}{L^2} - \frac{1}{4} F_{ab} F^{ab} - \frac{1}{4} Y_{ab} Y^{ab} - V(|\psi|) - |\partial\psi - iqA\psi|^2 \right], \quad (3.1)$$

which is a very simple extension of that introduced in [26, 27] for the balanced case. The Maxwell field A_a (resp. B_a) with field strength $F = dA$ (resp. $Y = dB$) is the holographic dual of the $U(1)_A$ “charge” (resp. $U(1)_B$ “spin”) current of the 2+1 dimensional field theory; when $Y = 0$ the system reduces to that introduced in [26, 27]. The metric is mapped into the field theory stress tensor. Finally, the complex scalar field ψ is dual to the condensate.

The action is chosen so that it admits an AdS_4 solution of radius L when all the matter fields are turned off. Since we are interested in finite temperature setups we will focus on asymptotically AdS_4 black hole solutions. Notice that the fields in the action are dimensionless and the gauge couplings have been reabsorbed in the overall gravitational constant κ_4^2 . Hence the $U(1)_A$ charge q of the scalar field has dimension of an energy.

The functional form of the potential $V(|\psi|)$ is not a priori constrained by the symmetries in the model. For simplicity, as in [26, 27], we will consider a potential containing only the mass term

$$V(|\psi|) = m^2 \psi^\dagger \psi. \quad (3.2)$$

By means of standard AdS/CFT map, the scalar field ψ results to be dual to a charged scalar operator of dimension

$$\Delta(\Delta - 3) = m^2 L^2. \quad (3.3)$$

With the aim of describing a fermionic Cooper pair-like condensate, $\mathcal{O}_\Delta = \Psi^T \Psi$ with canonical dimension $\Delta = 2$, we will mainly focus on a particular choice for the mass of the scalar field: $m^2 = -2/L^2$. Of course there is no reason to believe that this will be actually the dimension of the order parameter driving superconductivity at strong coupling, so we will also consider other mass values at $T = 0$. In any case the mass parameter will be taken to be above the Breitenlohner-Freedman (BF) bound in AdS_4 ,

$$m^2 L^2 \geq -\frac{9}{4}. \quad (3.4)$$

3.1 Ansatz and equations of motion

From the action (3.1) one obtains the following equations of motion: Einstein's equations

$$R_{ab} - \frac{g_{ab}R}{2} - \frac{3g_{ab}}{L^2} = -\frac{1}{2}T_{ab}, \quad (3.5)$$

where

$$\begin{aligned} T_{ab} = & -F_{ac}F_b^c - Y_{ac}Y_b^c + \frac{1}{4}g_{ab}F_{cd}F^{cd} + \frac{1}{4}g_{ab}Y_{cd}Y^{cd} \\ & + g_{ab}V(|\psi|) + g_{ab}|\partial\psi - iqA\psi|^2 \\ & - [(\partial_a\psi - iqA_a\psi)(\partial_b\psi^\dagger + iqA_b\psi^\dagger) + (a \leftrightarrow b)], \end{aligned} \quad (3.6)$$

Maxwell's equations for the A_a field

$$\frac{1}{\sqrt{-g}}\partial_a(\sqrt{-g}g^{ab}g^{ce}F_{bc}) = iqq^{ec}[\psi^\dagger(\partial_c\psi - iqA_c\psi) - \psi(\partial_c\psi^\dagger + iqA_c\psi^\dagger)], \quad (3.7)$$

the scalar equation

$$-\frac{1}{\sqrt{-g}}\partial_a[\sqrt{-g}(\partial_b\psi - iqA_b\psi)g^{ab}] + iqq^{ab}A_b(\partial_a\psi - iqA_a\psi) + \frac{1}{2}\frac{\psi}{|\psi|}V'(|\psi|) = 0, \quad (3.8)$$

and Maxwell's equations for the B_a field

$$\frac{1}{\sqrt{-g}}\partial_a(\sqrt{-g}g^{ab}g^{ce}Y_{bc}) = 0. \quad (3.9)$$

Let us now look for static asymptotically AdS black hole solutions of the previous equations. These solutions will be dual to the equilibrium phases of the dual quantum field theory.

For our purposes the most general ansatz for the spacetime metric is

$$ds^2 = -g(r)e^{-\chi(r)}dt^2 + \frac{r^2}{L^2}(dx^2 + dy^2) + \frac{dr^2}{g(r)}, \quad (3.10)$$

together with a homogeneous ansatz for the fields

$$\psi = \psi(r), \quad A_a dx^a = \phi(r)dt, \quad B_a dx^a = v(r)dt. \quad (3.11)$$

We will focus on black hole solutions, with a horizon at $r = r_H$ where $g(r_H) = 0$. The temperature of such black holes is given by

$$T = \frac{g'(r_H)e^{-\chi(r_H)/2}}{4\pi}. \quad (3.12)$$

Using one of Maxwell's equations we can safely choose ψ to be real. The scalar equation becomes

$$\psi'' + \psi' \left(\frac{g'}{g} + \frac{2}{r} - \frac{\chi'}{2} \right) - \frac{V'(\psi)}{2g} + \frac{e^{\chi} q^2 \phi^2 \psi}{g^2} = 0, \quad (3.13)$$

Maxwell's equations for the ϕ field become

$$\phi'' + \phi' \left(\frac{2}{r} + \frac{\chi'}{2} \right) - \frac{2q^2\psi^2}{g}\phi = 0, \quad (3.14)$$

the independent component of Einstein's equations yield

$$\frac{1}{2}\psi'^2 + \frac{e^\chi(\phi'^2 + v'^2)}{4g} + \frac{g'}{gr} + \frac{1}{r^2} - \frac{3}{gL^2} + \frac{V(\psi)}{2g} + \frac{e^\chi q^2 \psi^2 \phi^2}{2g^2} = 0, \quad (3.15)$$

$$\chi' + r\psi'^2 + r \frac{e^\chi q^2 \phi^2 \psi^2}{g^2} = 0, \quad (3.16)$$

Maxwell's equation for the v field becomes

$$v'' + v' \left(\frac{2}{r} + \frac{\chi'}{2} \right) = 0. \quad (3.17)$$

When $v(r) = 0$ these equations reduce to those found in [27]. As already mentioned we will specialize to the case where the scalar potential contains only the mass term. In appendix B we have reported the same equations of motion for a general dimension d of the spacetime. In the following we will work in units $L = 1$, $2\kappa_4^2 = 1$.

3.2 Boundary conditions

In order to find the solution to equations (3.13)–(3.17) one must impose two suitable boundary conditions: one in the interior of the spacetime at $r = r_H$ and one at the conformal boundary $r = \infty$, where we require AdS asymptotics. The analysis here is the standard one [26, 27]. At the horizon, both $g(r)$ and the temporal components of the gauge fields should be vanishing [26]. Hence we will require

$$\phi(r_H) = v(r_H) = g(r_H) = 0, \quad \text{and} \quad \psi(r_H), \chi(r_H) \text{ constants.} \quad (3.18)$$

The series expansions of the fields out of the horizon r_H , implementing the above boundary conditions, are the following

$$\phi_H(r) = \phi_{H1}(r - r_H) + \phi_{H2}(r - r_H)^2 + \dots, \quad (3.19)$$

$$\psi_H(r) = \psi_{H0} + \psi_{H1}(r - r_H) + \psi_{H2}(r - r_H)^2 + \dots, \quad (3.20)$$

$$\chi_H(r) = \chi_{H0} + \chi_{H1}(r - r_H) + \chi_{H2}(r - r_H)^2 + \dots, \quad (3.21)$$

$$g_H(r) = g_{H1}(r - r_H) + g_{H2}(r - r_H)^2 + \dots, \quad (3.22)$$

$$v_H(r) = v_{H1}(r - r_H) + v_{H2}(r - r_H)^2 + \dots \quad (3.23)$$

At the conformal boundary we must impose a leading behavior according to the corresponding dual boundary operators. Choosing $m^2 L^2 = -2$, the scalar field should approach the boundary in the following way

$$\psi(r) = \frac{C_1}{r} + \frac{C_2}{r^2} + \dots, \quad \text{as} \quad r \rightarrow \infty. \quad (3.24)$$

With a homogeneous ansatz (3.11) C_1 and C_2 are constants, independent on the field theory coordinates x_μ . Our choice of mass does not lead to non-normalizable modes

($-\frac{9}{4} < m^2 L^2 < -\frac{5}{4}$), hence we can in principle choose whether the leading or the sub-leading behavior in (3.24) should be the source of the dual operator \mathcal{O} . Since we want the condensate to arise spontaneously, we shall require either one or the other independent parameter in (3.24) to vanish. Specifically we will choose

$$C_1 = 0, \quad \langle \mathcal{O} \rangle = \sqrt{2} C_2, \tag{3.25}$$

where the factor $\sqrt{2}$ is a convenient normalization as in [26].

Vector fields at the boundary are given by

$$\phi(r) = \mu - \frac{\rho}{r} + \dots \quad \text{as } r \rightarrow \infty, \tag{3.26}$$

$$v(r) = \delta\mu - \frac{\delta\rho}{r} + \dots \quad \text{as } r \rightarrow \infty, \tag{3.27}$$

where μ (resp. ρ) and $\delta\mu$ (resp. $\delta\rho$) are the mean chemical potential (resp. the mean charge density) and the chemical potential mismatch (resp. the charge density mismatch) of the dual field theory.⁷ The reason behind the latter identifications has been explained before: a chemical potential mismatch can be realized by turning on a chemical potential for an effective $U(1)_s$ “spin” field, under which a Cooper-like order parameter (whose gravity dual is the scalar field ψ) is uncharged. The $U(1)_B$ Maxwell field (of which $v(r)$ is the electric component) is the holographic realization of such a field. Of course our gravity model just provides an effective description of the symmetries and the order parameters of the dual field theory. As such, the $U(1)_A$ and $U(1)_B$ fields that we treat as the holographic duals of the “charge” and the “spin” currents respectively, could be actually mapped into any couple of abelian global symmetries of which one can be broken by a vev of a charged scalar, while the other stays unbroken.

Notice that we work in units $L = 2\kappa_4^2 = 1$, where the bulk fields A_a, B_a and the parameters $\mu, \delta\mu$ have mass dimension 1, while ψ is dimensionless; ρ and $\delta\rho$ are charges per unit volume in the (2+1)-dimensional field theory, hence have dimension l^{-2} ; the radial coordinate r has dimension 1 in mass.

The functions in the metric ansatz should have AdS_4 asymptotics as in [27]

$$g(r) = r^2 - \frac{\epsilon}{2r} + \dots \quad \text{as } r \rightarrow \infty \tag{3.28}$$

$$\chi(r) = 0 + \dots \quad \text{as } r \rightarrow \infty, \tag{3.29}$$

where ϵ is holographically mapped to the energy density of the dual field theory.

4 The normal phase

A simple solution to the equations of motion (3.13)–(3.17) corresponds to the normal phase in the dual field theory. This is characterized by a vanishing vacuum expectation value of the condensate \mathcal{O} , corresponding to a vanishing scalar field $\psi = 0$ in the bulk. The

⁷In this paper we shall work in the grand-canonical ensemble with fixed chemical potentials.

corresponding background is that of a $U(1)^2$ -charged Reissner-Nordstrom- AdS_4 black hole, with metric

$$ds^2 = -f(r)dt^2 + r^2(dx^2 + dy^2) + \frac{dr^2}{f(r)}, \quad (4.1)$$

$$f(r) = r^2 \left(1 - \frac{r_H^3}{r^3}\right) + \frac{\mu^2 r_H^2}{4r^2} \left(1 - \frac{r}{r_H}\right) + \frac{\delta\mu^2 r_H^2}{4r^2} \left(1 - \frac{r}{r_H}\right). \quad (4.2)$$

Here r_H is the coordinate of the black hole outer horizon. The gauge fields are given by

$$\phi(r) = \mu \left(1 - \frac{r_H}{r}\right) = \mu - \frac{\rho}{r}, \quad (4.3)$$

$$v(r) = \delta\mu \left(1 - \frac{r_H}{r}\right) = \delta\mu - \frac{\delta\rho}{r}. \quad (4.4)$$

The temperature reads

$$T = \frac{r_H}{16\pi} \left(12 - \frac{\mu^2 + \delta\mu^2}{r_H^2}\right), \quad (4.5)$$

from which we get

$$r_H = \frac{2}{3}\pi T + \frac{1}{6}\sqrt{16\pi^2 T^2 + 3(\mu^2 + \delta\mu^2)}. \quad (4.6)$$

The Gibbs free energy density reads

$$\omega_n = -r_H^3 \left(1 + \frac{(\mu^2 + \delta\mu^2)}{4r_H^2}\right). \quad (4.7)$$

Notice that, due to formula (4.6), this is a function of T , μ and $\delta\mu$.

The doubly charged AdS black hole solution is certainly not new in the holographic condensed matter literature. For example, it also describes the normal phase of unbalanced p-wave superconductors [28]. As it was noticed in [13], the normal phase of a model like ours can be also seen as a rough holographic realization of a “forced” ferromagnet, where the “spin” density $\delta\rho$ is supported by a non zero value of $\delta\mu$ (and so, equivalently, by an external magnetic field). Indeed in our case $\delta\rho = 0$ if $\delta\mu = 0$.⁸

At $T = 0$ the doubly charged RN- AdS_4 black hole becomes extremal and (see equation (4.5)) the horizon radius reads

$$r_H^2 = \frac{1}{12}(\delta\mu^2 + \mu^2) \quad \text{at} \quad T = 0. \quad (4.8)$$

In the near-horizon limit the metric reduces to that of an $AdS_2 \times R^2$ background with AdS_2 radius given by $L_{(2)}^2 = L^2/6$ (see also appendix B).

The charge density imbalance at $T = 0$ reads

$$\delta\rho = \sqrt{\frac{\mu^2 + \delta\mu^2}{12}} \delta\mu. \quad (4.9)$$

⁸In a real ferromagnet, instead, the spin density $\delta\rho$ is spontaneously generated. Moreover there is a non vanishing ferromagnetic order parameter (a magnon). The holographic description of such a setup is an interesting open issue.

Notice that this is zero at $\delta\mu = 0$ as it happens for the normal phase at weak coupling (see appendix A). The susceptibility imbalance (“magnetic” susceptibility) reads thus

$$\delta\chi = \left. \frac{\partial\delta\rho}{\partial\delta\mu} \right|_{\delta\mu=0} = \frac{\mu}{\sqrt{12}}. \quad (4.10)$$

Therefore, in the limit $\delta\mu \ll \mu$, the Gibbs free energy density of the normal phase at $T = 0$ goes at leading order as

$$\omega(\delta\mu) \approx \omega(0) - \frac{1}{2} \frac{\mu}{\sqrt{12}} \delta\mu^2. \quad (4.11)$$

Following the same reasonings as in [4, 5] (see also appendix A), we can argue that, provided a superconducting phase exists at $T = 0$, *and it has $\delta\rho = 0$ for every $\delta\mu$* , a Chandrasekhar-Clogston bound at $T = 0$ should naturally arise also within the holographic setup.

Let us now ask whether there are conditions under which, lowering the temperature, a superconducting phase ($\psi \neq 0$) might arise with a formation of a charged condensate below a certain critical temperature T_c .

4.1 A criterion for instability

In our model we can find a simple condition (see also [13, 44]) on the external parameters in order for the normal phase to become unstable at $T = 0$. Let us consider a fluctuation of the complex scalar field ψ , charged under $U(1)_A$, around the extremal $U(1)^2$ -charged RN-AdS background. Its equation of motion has the form given in (3.13) with background metric given in (4.1) and $\phi(r)$ given in (4.3). The horizon radius is fixed as in (4.8).

In the near-horizon limit it is easy (see [44]) to see that the equation for ψ reduces to that of a scalar field of mass

$$m_{\text{eff}(2)}^2 = m^2 - \frac{2q^2}{\left(1 + \frac{\delta\mu^2}{\mu^2}\right)}, \quad (4.12)$$

on an AdS_2 background of squared radius $L_{(2)}^2 = 1/6$. The instability of the normal phase in this limit, is thus mapped into the requirement that the above effective mass is below the AdS_2 BF bound

$$L_{(2)}^2 m_{\text{eff}(2)}^2 = \frac{1}{6} m_{\text{eff}(2)}^2 < -\frac{1}{4}, \quad (4.13)$$

which leads to

$$\left(1 + \frac{\delta\mu^2}{\mu^2}\right) \left(m^2 + \frac{3}{2}\right) < 2q^2. \quad (4.14)$$

For an analogous formula in the general $d+1$ -dimensional case see appendix B (see also [13]).

When $(m^2 + \frac{3}{2}) < 0$, i.e. $m^2 < -\frac{3}{2}$, the instability occurs for every value of $\frac{\delta\mu^2}{\mu^2}$. This will indeed be the case for $m^2 = -2$. This suggests, quite surprisingly, that in these cases a superconducting phase with non-trivial scalar profile could be always preferred at $T = 0$, no matter how large is the chemical potential mismatch.⁹

⁹A similar result was found in [13] studying the instability of an extremal dyonic black hole, electrically and magnetically charged under a $U(1)$ field.

In the cases in which $(m^2 + \frac{3}{2}) > 0$, instead, the normal phase will show instability when

$$\frac{\delta\mu^2}{\mu^2} < 2q^2 \frac{1}{(m^2 + \frac{3}{2})} - 1, \tag{4.15}$$

which gives an actual bound on $\delta\mu/\mu$ provided that $4q^2 > 2m^2 + 3$. The above condition resembles the Chandrasekhar-Clogston bound of weakly interacting superconductors.

According to the comments in [45], we expect that a violation of the AdS_2 BF bound leads to a continuous phase transition of the Berezinskii-Kosterlitz-Thouless (BKT) type at $T = 0$ (see also [46]). In BKT transitions the order parameter goes to zero exponentially instead as with the power law behavior of second order phase transitions. Around these phase transitions there should be a turning point in the phase diagram, with the critical temperature slowly going to zero as an external parameter (for us $\delta\mu/\mu$) is increased. Actually, a BKT transition should become of second order at $T > 0$. Moreover, in [46] it has been observed that, in a holographic model, a BKT transition at $T = 0$ can only occur when the theory has two control parameters with the same dimension. This is precisely what happens in our case. Finally, notice that if the normal-to-superconducting phase transition at $T = 0$ is a continuous one (e.g. a BKT one) the critical value of the parameter $\delta\mu/\mu$ as deduced from the BF bound in AdS_2 should correspond to the critical value at which the phase transition occurs (see also analogous comments in [28]).

5 The superconducting phase

If the normal phase becomes unstable at low T , we must search for another static solution to the equations of motion (3.13)–(3.17) where the scalar field is non-zero. In the dual field theory this corresponds to turning on a vacuum expectation value of the condensate leading to a spontaneous symmetry breaking of an electromagnetic symmetry and the consequent emergence of a superconducting phase.

In the following we will discuss the results of a standard numerical analysis of the full set of equations of motion subjected to the boundary conditions discussed in section 3.2. The analysis is mainly based on the shooting technique and it is strictly valid at $T > 0$. We defer the study of the $T = 0$ case, along the lines considered in [44], to future work.

5.1 The condensate

Let us concentrate on what we can learn from the numeric solutions. First of all let us find an expression for the temperature as a function of the horizon values of the various fields. From the general expression (3.12) and the Einstein equation at the horizon, it follows that, for generic m^2

$$T = \frac{r_H}{16\pi} \left[(12 - 2m^2\psi_{H0}^2)e^{-\frac{\chi_{H0}}{2}} - \frac{1}{r_H^2} e^{\frac{\chi_{H0}}{2}} (\phi_{H1}^2 + v_{H1}^2) \right]. \tag{5.1}$$

The critical temperature is found by setting $\langle \mathcal{O} \rangle \sim C_2 = 0$.¹⁰

¹⁰A dimensionless combination involving T and the chemical potentials is $T/(\mu^2 + \delta\mu^2)^{1/2}$.

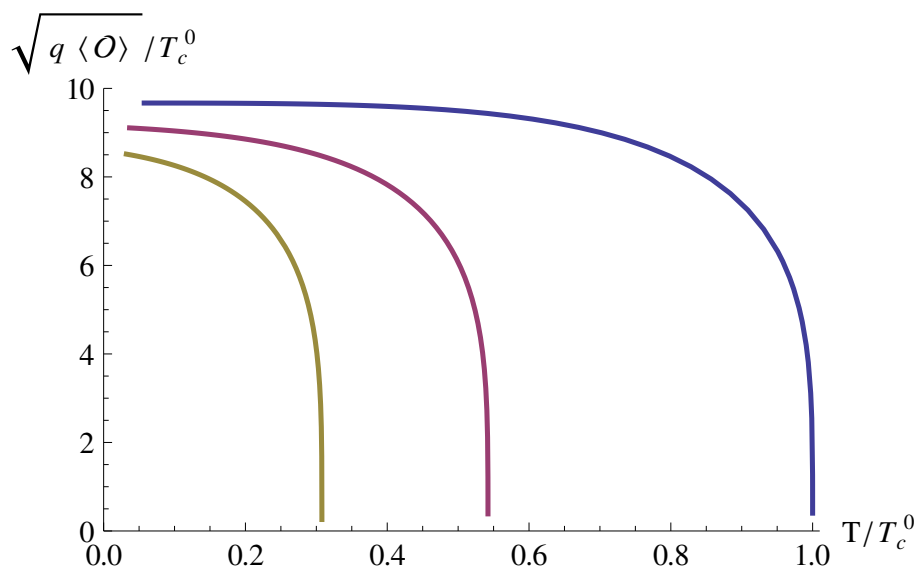


Figure 2. The value of the condensate as a function of the temperature at $\mu = 1, q = 2$. From right to left we have $\delta\mu = 0, 1, 1.5$ and the critical temperature is decreasing.

Our numerical analysis gives rise to the following results. For small values of the chemical potential mismatch $\delta\mu = 0.01$ and for different values of the external parameter q we obtain results similar to [27]. A condensate arises below a certain critical temperature T_c signaling a phase transition from a normal to a superconducting phase. The general form of these curves is similar to the ones in BCS theory, typical of mean field theories and second order phase transitions. The value of the condensate depends on the charge of the bulk field q . However, as in [27], it is difficult to get the numerics reliably down to very low temperatures.

Allowing for higher values of the chemical potential mismatch $\delta\mu$, we obtain analogous behaviors for the condensate. Increasing the value of $\delta\mu$ (see figure 2) we obtain a decreasing value of the critical temperature. The phase transition is always second order. The most interesting result is the plot of the critical temperature normalized to T_c^0 (the critical temperature at zero chemical potential mismatch), against $\delta\mu/\mu$. The second order phase transition at zero chemical potential mismatch develops inside the $(T_c, \delta\mu)$ phase diagram. As it is shown in figure 3, the critical temperature decreases with $\delta\mu/\mu$, a qualitative feature which we have seen also in the weakly coupled case. However, differently from the weakly coupled case, there is no finite value of $\delta\mu/\mu$ for which $T_c = 0$.¹¹ Hence, there is no sign of a Chandrasekhar-Clogston bound at zero temperature. This result matches with the expectations coming from the formula (4.14), which actually suggested the absence of such a bound for $m^2 = -2$. However, it should be desirable to refine our numerics around $T = 0$ as done in [44] to definitely confirm this conclusion. In any case, we believe that it is unlikely that the curve in figure 3 will suddenly drop to zero with another flex. The phase

¹¹A similar phase diagram appears in [47] in holographic superconductors in the presence of an external magnetic field.

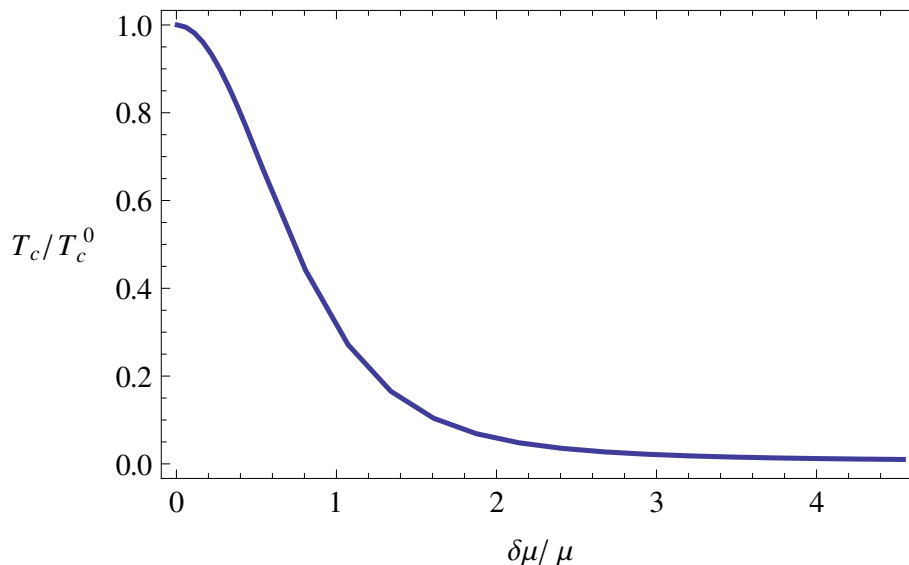


Figure 3. Second order phase transition line in the $(T_c, \delta\mu)$ plane with $q = 1$, $\mu = 1.87$. There are always values of T_c below which a superconducting phase arises.

transition we find is always second order as we have also checked by a standard holographic computation of the free energy along the same lines as in [27].¹² Together with the absence of a Chandrasekhar-Clogston bound, this leads us to argue that a LOFF phase is unlikely to develop.

5.2 Comments on the LOFF phase

Let us see whether the occurrence of inhomogeneous phases is actually forbidden in our model. For simplicity, we will limit our analysis to the so-called “probe” approximation as first considered in [26]. It consists in rescaling the scalar as well as the A_a gauge field by the charge $1/q$ and taking the $q \gg 1$ limit. In this way the backreaction of these fields on the metric can be neglected. This limit could only capture the physics at temperatures close to the critical temperature T_c , where the condensate (hence the field ψ) is actually small. In particular, it could be reliable around a tricritical point, in case this is displayed by the $(T, \delta\mu)$ phase diagram.

Looking for LOFF-like phases in this limit corresponds to looking for gravity solutions (on a fixed background) where the scalar field spontaneously acquires a dependence on e.g. one of the spatial directions. In particular we will focus on complex one-plane wave solutions and on real sinusoidal ones.¹³ In our case the fixed background is given by a

¹²Notice that, as we have previously argued, the phase diagram could change for different choices of the mass parameters in our model. We defer this analysis to future works.

¹³Inhomogeneous phases of this kind in holographic p-wave superconductors have been considered in, e.g. [31–33, 48].

U(1)_B-charged RN-AdS black hole

$$ds^2 = -f(r)dt^2 + r^2(dx^2 + dy^2) + \frac{dr^2}{f(r)}, \quad (5.2)$$

$$f(r) = r^2 \left(1 - \frac{r_H^3}{r^3}\right) + \frac{\delta\mu^2 r_H^2}{4r^2} \left(1 - \frac{r}{r_H}\right), \quad (5.3)$$

$$v_t = \delta\mu \left(1 - \frac{r_H}{r}\right) = \delta\mu - \frac{\delta\rho}{r}. \quad (5.4)$$

Let us now consider a simple single plane wave inhomogeneous ansatz

$$\psi(r, x) = \Psi(r)e^{-ixk}, \quad A = A_t(r)dt + A_x(r)dx. \quad (5.5)$$

Inserting the above ansatz in the equations of motion (3.7) and (3.8) on the fixed U(1)_B-charged RN-AdS background (5.2), (5.3), (5.4), one gets Maxwell's equations

$$\partial_r^2 A_t + \frac{2}{r} \partial_r A_t - \frac{2\Psi^2}{f} A_t = 0, \quad (5.6)$$

$$\partial_r^2 A_x + \frac{f'}{f} \partial_r A_x - \frac{2\Psi^2}{f} (k + A_x) = 0, \quad (5.7)$$

and the scalar equation

$$\Psi'' + \Psi' \left(\frac{2}{r} + \frac{f'}{f}\right) + \Psi \left(\frac{A_t^2}{f^2} + \frac{2}{f} - \frac{(k + A_x)^2}{r^2 f}\right) = 0. \quad (5.8)$$

These equations always admit a trivial solution with $A_x = -k$ which is just related to the $k = 0$ one by bulk gauge transformations. Both solutions thus correspond to the same zero-current homogeneous phase. In order to find non-trivial solutions corresponding to an absolute equilibrium state with zero superfluid current¹⁴ we could require the Maxwell field $A_x(r)$ to have UV boundary conditions such that

$$A_x(r \rightarrow \infty) \approx -k + \frac{J}{r}, \quad \text{with } J = 0. \quad (5.9)$$

The large- r asymptotics for Ψ and A_t are taken as in the homogeneous case. From the above equations it is easy to realize that non-trivial solutions for A_x satisfying the boundary condition (5.9) are not admitted. This is true for generic values of m^2 , for which the scalar field $\Psi(r)$, dual to the same kind of operator we have considered above, has to go like $\Psi \approx Cr^{-\lambda}$ at large r (here $\lambda = (3 + \sqrt{9 + 4m^2})/2$ is the operator UV dimension). The same conclusion is reached starting from a more general ansatz in which $A_t = A_t(x, r)$ and $A_x = A_x(x, r)$, with the same large r asymptotics as in (5.9). Maxwell's equations in this case imply separability $\partial_x \partial_r A_x = 0$ and consistency forces A_x and A_t to lose their dependence on x , thus reducing the setup to the one above.

It is also possible to show that two-wave real condensates going like $\psi = \Psi(r) \cos(kx)$ are excluded already at the level of the equations of motion.

All in all, this analysis seems to exclude the possibility that a LOFF-like phase, and thus a related tricritical point in the $(T, \delta\mu)$ phase diagram, can be displayed by our model.

¹⁴This is a necessary condition for having a LOFF ground state [2, 3] and it marks a difference w.r.t. the standard superfluid phases with non zero superfluid velocity, see e.g. [49–52].

6 Conductivities: holographic spintronics

In this section we present the study of the conductivities of the system as functions of the frequency of the applied external field perturbations. In this paper we limit the analysis to zero-momentum perturbations. Thanks to the rotational invariance of the theory in the $x - y$ plane, it is sufficient to consider the conductivities in one direction, say along x . According to the AdS/CFT dictionary, the calculation is performed through the study of the response of the gravity system to vector perturbations in the x direction. The holographic computation, which is fairly standard, is described in section 6.2; the uninterested reader can safely skip it (apart from formulas (6.20), (6.21), (6.23)) and go to the results in sections 6.3 and 6.4.

6.1 The conductivity matrix

The system at hands includes two U(1) vector fields describing two currents of the dual boundary theory. As mentioned in the Introduction, it represents a minimal holographic description of the “two-current model” [8–12] which lies at the roots of the theoretical study of spintronics. The two-current model is based on the observation by Mott [8, 9] that at low temperature the two currents of spin “up” and “down” electrons can be considered as two separate entities, with two corresponding conductivities which are in principle different. The system is typically a ferromagnetic metal with a non zero spin polarization $\delta\rho$.

In such case, an applied external electric field E^c (providing an “electric motive force”) does not generate only an electric current J^c with conductivity σ_{cc} , but can also generate a net spin current J^s . The corresponding conductivity is sometimes called (somehow asymmetrically) the “spin conductivity” σ_{cs} . Moreover, this effect is reciprocal: a “spin motive force” generated by an external applied field E^s (essentially, a dynamical gradient of population imbalance,¹⁵ $\nabla\delta\mu$), on top of creating a spin current J^s with conductivity σ_{ss} (we call this the “spin-spin conductivity”), induces an electric current J^c as well, with conductivity σ_{sc} [11, 12]; the latter is precisely equal to the spin conductivity σ_{cs} in time-reversal invariant settings. We will not consider dissipative effects bringing to spin-relaxation in this paper.

The electric and spin motive forces can be described by means of two U(1) gauge fields: the electro-magnetic one and the spin one; the latter is an effective gauge boson. In this paper we have presented a gravity theory which precisely encodes the minimal ingredients of a macroscopic description of the two-current model: a charged environment, i.e. the charged black hole, with two vector operators, dual to the two gauge fields A_a and B_a . The two gauge fields are not directly coupled in the gravity Lagrangian, but their fluctuations are coupled via their coupling with the metric. As a result, the two dual currents are coupled through their mixing with the energy-momentum tensor operator of the field theory. Obviously enough, there is a mixing with the heat current as well.

¹⁵This can be generated by “dynamical magnetic textures”, e.g. dynamical magnetizations in ferromagnetic conductors. Typical potential differences are generated by appropriately engineered sequences of layers of materials with different magnetic properties. Thus, the “spin motive force” is generated perpendicularly to the layers. In our gravity dual model, we instead consider the “spin motive force” in the plane; for our purposes the difference of the two settings is irrelevant.

Thus, we would like to stress the fact that from the dual gravitational point of view, the mixing of the two current operators, which causes the crucial existence of the “spin conductivity” $\sigma_{cs} = \sigma_{sc}$, is completely straightforward and universal. In fact, both currents bring some momentum, thus they source the momentum operator T_{tx} ; the latter is dual to the metric component g_{tx} which, being a vector perturbation of the metric, mixes with both gravity vector fields, coupling the dual operators. In other words, this phenomenon is not very sensitive to the details of the gravity Lagrangian used to describe the two-current model: generally, a gravity theory with two conserved U(1)’s will provide a non-zero dual “spin conductivity”.

Furthermore, the gravity theory at hands includes a charged operator (under the “electric charge”) which condenses at sufficiently small temperature. Thus, the system describes both the normal phase of a two-current model, and a superconducting phase thereof. It must also be remembered that the gravity theory provides a dual description of strongly interacting microscopic degrees of freedom, as opposed to the usual weakly interacting fermion systems of the standard spintronics literature.

Actually, the gravity description does not rely on the specific microscopic origin of the two U(1) currents in terms of charge and spin, although it describes the same basic features. In this sense, it is more “universal” and could be possibly applied to other microscopic theories, such as QCD-like ones. Thus, we chose to call J^A, E^A, σ_A the current, external field and conductivity associated to the $U(1)_A$ under which the scalar operator is charged; these are the quantities which we called “electric” above (i.e. electric current J^c , field E^c , conductivity σ_{cc}). Analogously, we call J^B, E^B, σ_B the quantities associated to the $U(1)_B$ under which the scalar operator is un-charged; above we referred to them in relation to the “spin” (i.e. they are J^s, E^s, σ_{ss} in the case of electron spin unbalance). Finally, we name γ the mixed conductivity ($\sigma_{cs} = \sigma_{sc}$ above). Nevertheless, in the discussion below we will often indulge with the “electric/spin” terminology for a (hopefully) clearer presentation.

According to the discussion above, all the conductivities are included in the general non-diagonal matrix (see e.g. [11, 12] and [27] for the notation)

$$\begin{pmatrix} J^A \\ Q \\ J^B \end{pmatrix} = \begin{pmatrix} \sigma_A & \alpha T & \gamma \\ \alpha T & \kappa T & \beta T \\ \gamma & \beta T & \sigma_B \end{pmatrix} \cdot \begin{pmatrix} E^A \\ -\frac{\nabla T}{T} \\ E^B \end{pmatrix}. \tag{6.1}$$

In this matrix, σ_A, σ_B are the diagonal conductivities associated to the two U(1)’s. In the language used above, the former is the standard electric conductivity, measuring the proportionality between an applied external electric field E^A and a generated electric current J^A . Analogously, the “spin-spin” conductivity σ_B is the proportionality coefficient between a gradient in the imbalance chemical potential $\delta\mu$ (which we called E^B above to underline the similarity with E^A), and the generated spin current J^B . The third diagonal entry in (6.1), κ , is the thermal conductivity, i.e. the proportionality between the thermal gradient $-\frac{\nabla T}{T}$ and the heat current $Q = T_{tx} - \mu J^A - \delta\mu J^B$.

Moreover, α and β are the thermo-electric and “thermo-spin” conductivities;¹⁶ they are associated to the transport of heat in the presence of an electric, or spin, potential

¹⁶ β is sometimes called the “thermo-magnetic” conductivity [11, 12].

even without a temperature gradient ∇T . Finally, γ measures e.g. the spin current J^B generated by an applied electric potential E^A even without an applied external field E^B .

The matrix (6.1) is symmetric because of time-reversal symmetry [11, 12, 27].

6.2 Holographic calculation of the conductivities

We follow closely the presentation in [26, 27] throughout all the present section, underlining the novelties of the unbalanced case. In the holographic approach, the fluctuations of the fields A_x, B_x, g_{tx} at the AdS boundary, act as sources for the currents J_x^A, J_x^B and the stress energy tensor component T_{tx} . Conductivity is a transport phenomenon, hence it requires a real time description. Since the black hole solutions we consider are classical, we must require in-going boundary conditions for the fields A_x, B_x, g_{tx} at the horizon. Let us take a simple $e^{-i\omega t}$ time dependence for the fluctuations and consider the related linearized Einstein and Maxwell equations on the background

$$A_x'' + \left(\frac{g'}{g} - \frac{\chi'}{2}\right) A_x' + \left(\frac{\omega^2}{g^2} e^\chi - \frac{2q^2\psi^2}{g}\right) A_x = \frac{\phi'}{g} e^\chi \left(-g'_{tx} + \frac{2}{r} g_{tx}\right), \quad (6.2)$$

$$B_x'' + \left(\frac{g'}{g} - \frac{\chi'}{2}\right) B_x' + \frac{\omega^2}{g^2} e^\chi B_x = \frac{v'}{g} e^\chi \left(-g'_{tx} + \frac{2}{r} g_{tx}\right), \quad (6.3)$$

$$g'_{tx} - \frac{2}{r} g_{tx} + \phi' A_x + v' B_x = 0. \quad (6.4)$$

The prime represents the derivative with respect to the bulk radial coordinate r . Substituting (6.4) into (6.2) and (6.3) we obtain

$$A_x'' + \left(\frac{g'}{g} - \frac{\chi'}{2}\right) A_x' + \left(\frac{\omega^2}{g^2} e^\chi - \frac{2q^2\psi^2}{g}\right) A_x - \frac{\phi'}{g} e^\chi (B_x v' + A_x \phi') = 0, \quad (6.5)$$

$$B_x'' + \left(\frac{g'}{g} - \frac{\chi'}{2}\right) B_x' + \frac{\omega^2}{g^2} e^\chi B_x - \frac{v'}{g} e^\chi (B_x v' + A_x \phi') = 0. \quad (6.6)$$

In this way we can deal with two equations in which the metric fluctuations do not appear. Notice that the substitution has lead to a system of linear differential equations in which the two gauge fields A_x and B_x are mixed. It is important to underline the rôle of the metric in such mixing: indeed, in the probe approximation, no coupling between the different gauge fields occurs.

In order to solve (6.5) and (6.6), we assume the following near-horizon behavior ansatz for the fluctuation functions¹⁷

$$A_x(r) = \left(1 - \frac{r_H}{r}\right)^{i\omega} \left[a_0 + a_1 \left(1 - \frac{r_H}{r}\right) + \dots \right], \quad (6.7)$$

$$B_x(r) = \left(1 - \frac{r_H}{r}\right)^{i\omega} \left[b_0 + b_1 \left(1 - \frac{r_H}{r}\right) + \dots \right]. \quad (6.8)$$

The IR solution depends on two integration constants, a_0, b_0 . The overall scaling symmetry ($A_x \rightarrow \lambda A_x, B_x \rightarrow \lambda B_x$) of equations (6.5), (6.6) allows one to fix e.g. $a_0 = 1$.

¹⁷It can be checked that in order to have a non-trivial solution of the equations around the horizon, the frequencies of the two modes must be equal. Moreover, inspection of the behavior of the equations near the horizon dictates that the exponential coefficients “ a ” of the leading terms of the two modes must be equal too.

In the UV, the behavior of the fields is

$$A_x(r) = A_x^{(0)} + \frac{1}{r}A_x^{(1)} + \dots, \quad (6.9)$$

$$B_x(r) = B_x^{(0)} + \frac{1}{r}B_x^{(1)} + \dots, \quad (6.10)$$

$$g_{tx}(r) = r^2 g_{tx}^{(0)} - \frac{1}{r}g_{tx}^{(1)} + \dots. \quad (6.11)$$

With this notation, the solution for g_{tx} in equation (6.4) can be expressed as

$$g_{tx} = r^2 \left(g_{tx}^{(0)} + \int_r^\infty \frac{\phi' A_x + v' B_x}{r^2} \right), \quad (6.12)$$

so that

$$g_{tx}^{(1)} = \frac{\rho}{3} A_x^{(0)} + \frac{\delta\rho}{3} B_x^{(0)}. \quad (6.13)$$

Moreover, from linearity and symmetries of (6.5) and (6.6) it follows that, on-shell,

$$A_x^{(1)} = i\omega\sigma_A A_x^{(0)} + i\omega\gamma B_x^{(0)}, \quad B_x^{(1)} = i\omega\gamma A_x^{(0)} + i\omega\sigma_B B_x^{(0)}, \quad (6.14)$$

where the reason behind the labeling of the ω -dependent coefficients will be clear in a moment.

The linear response of a current J^a to perturbations $\sum_b \phi_b J^b$ driven by external sources ϕ_b is given in terms of retarded correlators. Formally, in momentum space, $\langle J^a \rangle = G_R[J^a, J^b]\phi_b$. In our case, the retarded correlators G_R , which are proportional to the conductivities, can be holographically computed using the on-shell gravity action for the dual fields as generating functional. The on-shell action for the quadratic fluctuations of A_x, B_x, g_{tx} can be expressed as just a boundary term at infinity and, after performing the holographic renormalization procedure, it can be reduced to [27]

$$S_{quad} = \int d^3x \left(\frac{1}{2} A_x^{(0)} A_x^{(1)} + \frac{1}{2} B_x^{(0)} B_x^{(1)} - 3g_{tx}^{(0)} g_{tx}^{(1)} - \frac{\epsilon}{2} g_{tx}^{(0)} g_{tx}^{(0)} \right), \quad (6.15)$$

with $A_x^{(1)}, B_x^{(1)}, g_{tx}^{(1)}$ given in (6.13) and (6.14).

The conductivity matrix can be thus deduced using the holographic relations

$$J^A = \frac{\delta S_{quad}}{\delta A_x^{(0)}}, \quad (6.16)$$

$$J^B = \frac{\delta S_{quad}}{\delta B_x^{(0)}}, \quad (6.17)$$

$$Q = \frac{\delta S_{quad}}{\delta g_{tx}^{(0)}} - \mu J^A - \delta\mu J^B, \quad (6.18)$$

provided the following formulas (see Hartnoll's and Herzog's reviews in [16–22] for details) are employed

$$E_x^A = i\omega(A_x^{(0)} + \mu g_{tx}^{(0)}), \quad E_x^B = i\omega(B_x^{(0)} + \delta\mu g_{tx}^{(0)}), \quad -\frac{\nabla_x T}{T} = i\omega g_{tx}^{(0)}. \quad (6.19)$$

We can thus get

$$\begin{aligned}
 \sigma_A &= \frac{J^A}{EA} \Big|_{g_{tx}^{(0)}=B_x^{(0)}=0} = -\frac{i}{\omega} \frac{A_x^{(1)}}{A_x^{(0)}} \Big|_{g_{tx}^{(0)}=B_x^{(0)}=0}, \\
 \gamma &= \frac{J^B}{EA} \Big|_{g_{tx}^{(0)}=B_x^{(0)}=0} = -\frac{i}{\omega} \frac{B_x^{(1)}}{A_x^{(0)}} \Big|_{g_{tx}^{(0)}=B_x^{(0)}=0}, \\
 \alpha T &= \frac{Q}{EA} \Big|_{g_{tx}^{(0)}=B_x^{(0)}=0} = \frac{i\rho}{\omega} - \mu\sigma_A - \delta\mu\gamma,
 \end{aligned} \tag{6.20}$$

as well as

$$\begin{aligned}
 \sigma_B &= \frac{J^B}{EB} \Big|_{g_{tx}^{(0)}=A_x^{(0)}=0} = -\frac{i}{\omega} \frac{B_x^{(1)}}{B_x^{(0)}} \Big|_{g_{tx}^{(0)}=A_x^{(0)}=0}, \\
 \gamma &= \frac{J^A}{EB} \Big|_{g_{tx}^{(0)}=A_x^{(0)}=0} = -\frac{i}{\omega} \frac{A_x^{(1)}}{B_x^{(0)}} \Big|_{g_{tx}^{(0)}=A_x^{(0)}=0}, \\
 \beta T &= \frac{Q}{EB} \Big|_{g_{tx}^{(0)}=A_x^{(0)}=0} = \frac{i\delta\rho}{\omega} - \delta\mu\sigma_B - \mu\gamma.
 \end{aligned} \tag{6.21}$$

Notice the relation

$$\gamma = \sigma_A \frac{J^B}{J^A} \Big|_{g_{tx}^{(0)}=B_x^{(0)}=0} = \sigma_B \frac{J^A}{J^B} \Big|_{g_{tx}^{(0)}=A_x^{(0)}=0}, \tag{6.22}$$

which constitutes a valuable test in the numerical calculations.

Finally, we find that the (non canonical) thermal conductivity is given by

$$\kappa T = \frac{i}{\omega} [\epsilon + p - 2\mu\rho - 2\delta\mu\delta\rho] + \sigma_A\mu^2 + \sigma_B\delta\mu^2 + 2\gamma\mu\delta\mu, \tag{6.23}$$

where the term in the pressure $p = \epsilon/2$ has been added by hand to account for contact terms not directly implemented by the previous computations (see Herzog’s review in [16–22]).

The relations we have found between the different conductivities emerge quite naturally from the holographic setup. In the dual field theories they arise from Ward identity constraints on the correlators (see, again, Herzog’s review).

Solving numerically the equations (6.5), (6.6) for the fluctuations of A_x and B_x and using the formulas above, we can calculate all the conductivities ($\sigma_A, \sigma_B, \gamma, \kappa, \alpha T, \beta T$) in terms of values of the dual gravity fields.¹⁸

6.3 Conductivities in the normal phase

As we have noticed in section 4, following [13], the normal phase of our model can be seen as a simplified holographic realization of a “forced” ferromagnet. Studying the conductivity matrix in this case is thus quite interesting, since it allows us to make some parallel with known results in ferromagnetic spintronics.

In the left plot of figure 4 we present the results for the real part of σ_A (the optical electric conductivity) as a function of the frequency of the external field perturbation for vanishing imbalance, $\delta\mu = 0$, i.e. the case considered in [27]. The different curves

¹⁸An alternative method consists in considering the linear relations in (6.1) for different arbitrary choices of the values of the fluctuations at the horizon, in order to obtain enough equations to determine the various conductivities. Solving the system numerically we have checked that this method is stable w.r.t. those choices and it gives the same results as the method described above.

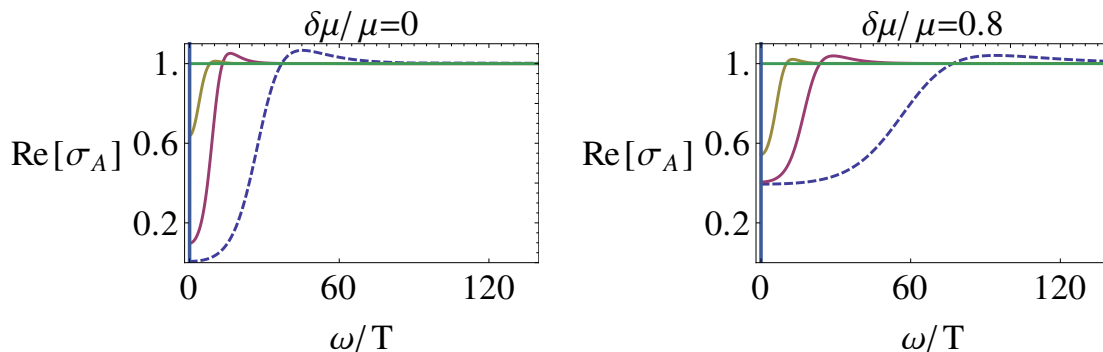


Figure 4. The real part of the electric conductivity for $\delta\mu/\mu = 0, 0.8$ (left plot, right plot) at T_c (dashed curves) and $T > T_c$ (solid curves).

correspond to different temperatures; the dashed curve is at the critical temperature for the onset of superconductivity. At very large temperature, the conductivity is basically constant (quantities are normalized such that the constant is precisely equal to 1); this feature is peculiar of the gravity description we are using.¹⁹

As the temperature is decreased, the conductivity is depleted at small frequencies. In fact, the imaginary part of σ_A (not shown) has a pole at $\omega = 0$; this is mapped by a Kramers-Kronig relation to a delta function for $\text{Re}[\sigma_A]$ at the same point (the solid line at $\omega/T = 0$ in the figure). The delta function at zero frequency is due to the system translation invariance which, in charged media, causes an overall uniform acceleration and so an infinite DC conductivity.²⁰ Since the area under the curves must be constant at different temperatures due to a Ferrell-Glover-Tinkham sum rule, the development of a delta function at $\omega = 0$ is compensated by a depletion of the conductivity at small frequencies [27].

In the right plot of figure 4 we present the results for the real part of σ_A for non-vanishing imbalance, $\delta\mu/\mu = 0.8$. The general trend is clearly the same as in the balanced case. Nevertheless, the depth of the depletion at small frequencies is reduced with respect to the $\delta\mu/\mu = 0$ case (remember that T_c is reduced too): the magnitude of the delta function is reduced, i.e. the DC conductivity is decreased by $\delta\mu$.

Concerning the real part of σ_B (the “optical spin-spin conductivity”), it is exactly constant in absence of imbalance, $\delta\mu = 0$: there is no “net spin” in the system, so the conductivity is featureless.²¹ The unbalanced case, $\delta\mu/\mu = 0.8$, is reported in the left plot of figure 5. The similarity with the plot of σ_A , including the infinite DC conductivity, is transparent. In fact, it is clear (for example from equations (6.5), (6.6)) that in the normal phase (that is, at zero ψ) the system enjoys the symmetry

$$\sigma_A(\mu, \delta\mu, \omega/T) = \sigma_B(\delta\mu, \mu, \omega/T), \quad (6.24)$$

¹⁹It depends on electro-magnetic duality of the four-dimensional Einstein-Maxwell theory on AdS_4 [53].

²⁰This infinity is of course expected to transform into the standard Drude peak upon inclusion of impurities breaking translation invariance. Note that we are working with the fully backreacted solution, so there is no dissipation as it happens in the probe limit, and as a result translational invariance is preserved.

²¹The gravity vector B_a fluctuates on a black hole background charged under the other $U(1)_A$.

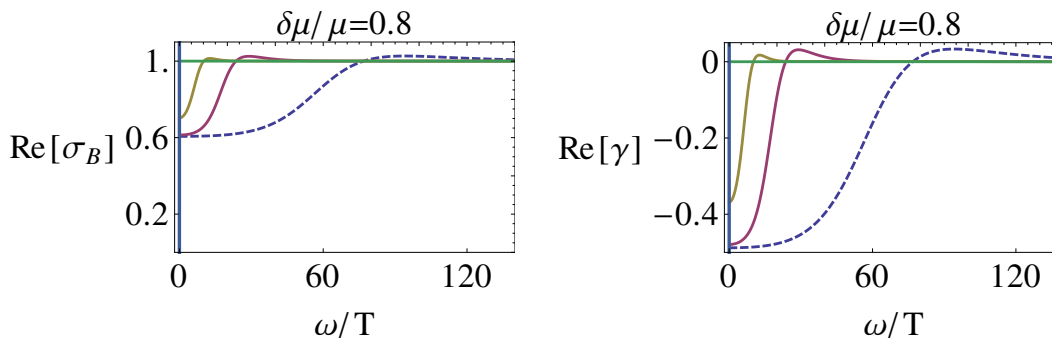


Figure 5. The real part of the “spin-spin conductivity” σ_B (left) and of the “spin conductivity” γ (right) for $\delta\mu/\mu = 0.8$ at T_c (dashed curves) and $T > T_c$ (solid curves).

which we also verified numerically with $\mathcal{O}(10^{-3})$ accuracy (at least). In particular,

$$\sigma_A = \sigma_B \quad \text{for} \quad \mu = \delta\mu. \quad (6.25)$$

This is the same as stating that for perfectly polarized electrons (say all spins “up”), the electric conductivity σ_{cc} (σ_A) equals the “spin-spin” one σ_{ss} (σ_B). In this case, then, we recover the zero-momentum result in [14, 15].

Actually, formula (6.24) is just a part of a set of more general relations among the various conductivities in the normal phase. In fact, it turns out that all the conductivities can be given once a single frequency dependent function $f = f(\omega/T, \delta\mu/\mu)$ (a “mobility function” for the charge/spin carriers) is known. Considering formulas (6.20), (6.21), (6.23), the conductivity matrix $\hat{\sigma}$ in the normal phase turns out to be²²

$$\begin{aligned} \hat{\sigma} &= \begin{pmatrix} \sigma_A & \alpha T & \gamma \\ \alpha T & \kappa T & \beta T \\ \gamma & \beta T & \sigma_B \end{pmatrix} \\ &= \begin{pmatrix} f\rho^2 + 1 & \frac{i\rho}{\omega} - \mu(f\rho^2 + 1) - \delta\mu f\rho\delta\rho & f\rho\delta\rho \\ \frac{i\rho}{\omega} - \mu(f\rho^2 + 1) - \delta\mu f\rho\delta\rho & \kappa T & \frac{i\delta\rho}{\omega} - \delta\mu(f\delta\rho^2 + 1) - \mu f\rho\delta\rho \\ f\rho\delta\rho & \frac{i\delta\rho}{\omega} - \delta\mu(f\delta\rho^2 + 1) - \mu f\rho\delta\rho & f\delta\rho^2 + 1 \end{pmatrix}. \end{aligned} \quad (6.26)$$

These relations concern both the real and the imaginary parts of the conductivities. The matrix (6.26) reproduces in many instances the expectations in [11, 12], for example despite their complicated explicit expressions, we have $\beta T = (\delta\rho/\rho)\alpha T$ (since in the normal phase $\rho\delta\mu = \mu\delta\rho$, see section 4). The diagonal conductivities are related quadratically to the corresponding charge densities because the more the carriers are coupled the more they feel the external field, and, in addition, the bigger the charge density the stronger the transport. Again, the form (6.26) has been verified numerically with at least $\mathcal{O}(10^{-3})$ accuracy.

The right plot of figure 5 reports the results for γ , the mixed conductivity (the “spin conductivity” $\sigma_{sc} = \sigma_{cs}$), at $\delta\mu/\mu = 0.8$. At $\delta\mu = 0$ this conductivity is identically zero: in absence of “net spin”, an external electric field does not cause the transport of “spin”

²²We have left κT implicit just to save space: its expression, in terms of the other conductivities and of the thermodynamical parameters in the normal phase (as given in section 4) can be immediately deduced from eq. (6.23).

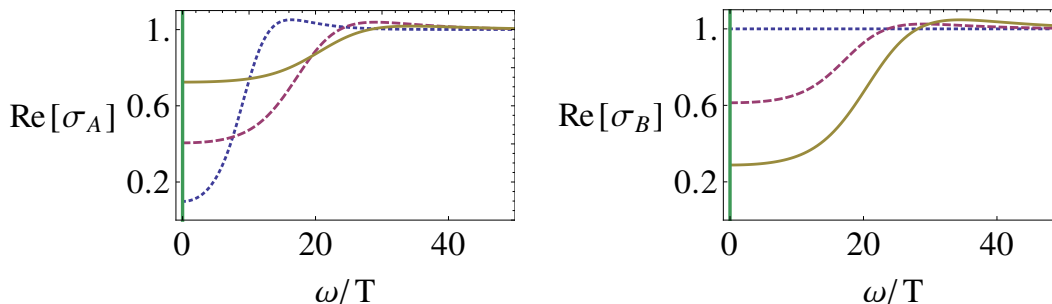


Figure 6. The real part of the electric conductivity σ_A (left) and of the “spin-spin conductivity” σ_B (right) for $\delta\mu/\mu = 0, 0.8, 1.6$ (dotted, dashed and solid lines respectively) at fixed temperature.

(and the other way around). Instead, as $\delta\mu/\mu \neq 0$, we have the typical phenomenon at the roots of spintronics: an external electric field causes the transport of “spin” (and the other way around) with a non-trivial conductivity γ .

Note that in the $\mu = \delta\mu$ case (which from formulas (4.3), (4.4) is equivalent to $\rho = \delta\rho$), (6.26) implies $\gamma = \sigma_A - 1 = \sigma_B - 1$: for perfectly polarized electrons the “spin conductivity” γ is equal to the electric conductivity σ_A , except for the constant contribution at large ω/T (the “1” in formula (6.26) with our normalizations of the constant conductivity). The latter contribution marks the difference with the quasi-free electron case recently studied in [14, 15], where $\gamma = \sigma_B$ at $\mu = \delta\mu$. The discrepancy is simply due to the fact that, differently from the quasi-free electron case, in the system at hand we have conduction even in the absence of net charge/spin density.

In figure 6 we present the real part of σ_A (left) and σ_B (right) at fixed temperature for different values of $\delta\mu/\mu = 0, 0.8, 1.6$ (dotted, dashed and solid lines respectively).²³ Note the opposite behavior, dictated by formula (6.24), of the conductivities σ_A, σ_B with increasing $\delta\mu/\mu$, which determines the increase of the σ_B DC conductivity with $\delta\mu/\mu$. This behavior, which has obvious physical origin in our system, is present in other contexts as well (see e.g. [54]), where it is usually interpreted as a separation of the dynamics of charge and spin degrees of freedom.

In figure 7 we present the real part of γ (left) and of the thermal conductivity κ (right) at fixed temperature for different values of $\delta\mu/\mu = 0, 0.8, 1.6$ (dotted, dashed and solid lines respectively). Notice the non-monotonic behavior with $\delta\mu/\mu$ of both $\text{Re}[\gamma]$ and $\text{Re}[\kappa]$ in the small frequency region. Notice moreover that there is a delta function (whose coefficient is enhanced by $\delta\mu$) in the DC thermal conductivity due to momentum conservation (translation invariance) which forbids the relaxation of the heat current [27]. This is reflected in a pole in $\text{Im}[\kappa]$ at $\omega = 0$.

Finally, in figure 8 we report the real part of the thermo-electric conductivity αT (left) and of the “spin-electric” conductivity βT (right) at fixed temperature for different values of $\delta\mu/\mu = 0, 0.8, 1.6$ (dotted, dashed and solid lines respectively).

²³We consider a generic setup where $\delta\mu/\mu$ is not constrained to be smaller or equal to one. In QCD with up-down quark condensates, for example, $\delta\mu$ is given by the isospin chemical potential, while μ is the baryonic one, the two being in principle independent.

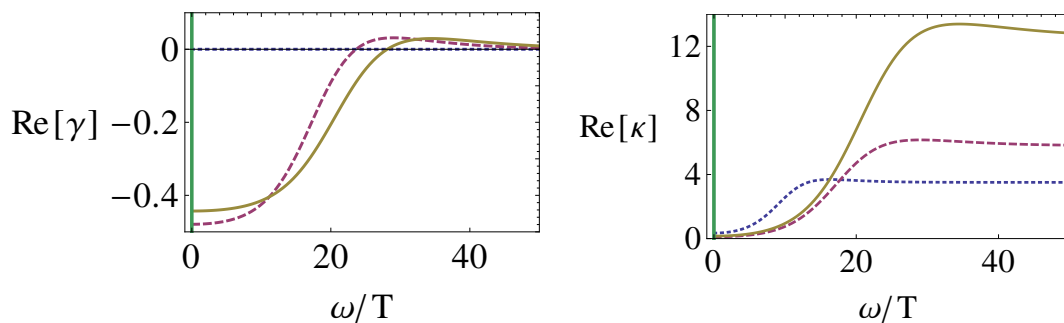


Figure 7. The real part of the “spin conductivity” γ (left) and of the thermal conductivity κ (right) for $\delta\mu/\mu = 0, 0.8, 1.6$ (dotted, dashed and solid lines respectively) at fixed temperature.

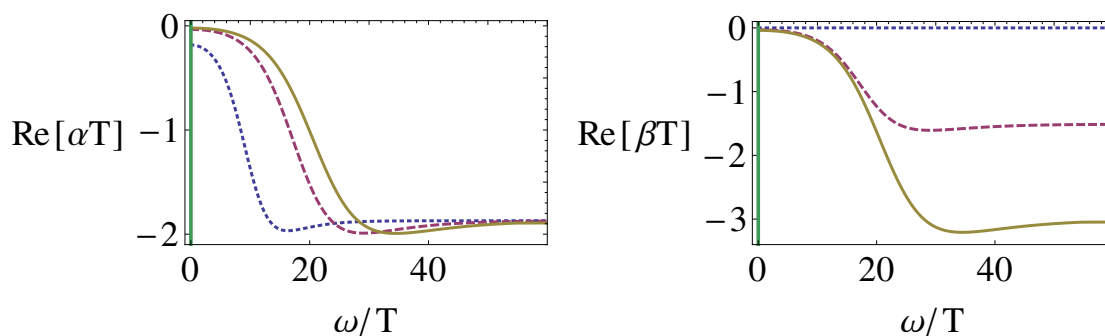


Figure 8. The real part of the thermo-electric conductivity αT (left) and of the “spin-electric” conductivity βT (right) for $\delta\mu/\mu = 0, 0.8, 1.6$ (dotted, dashed and solid lines respectively) at fixed temperature.

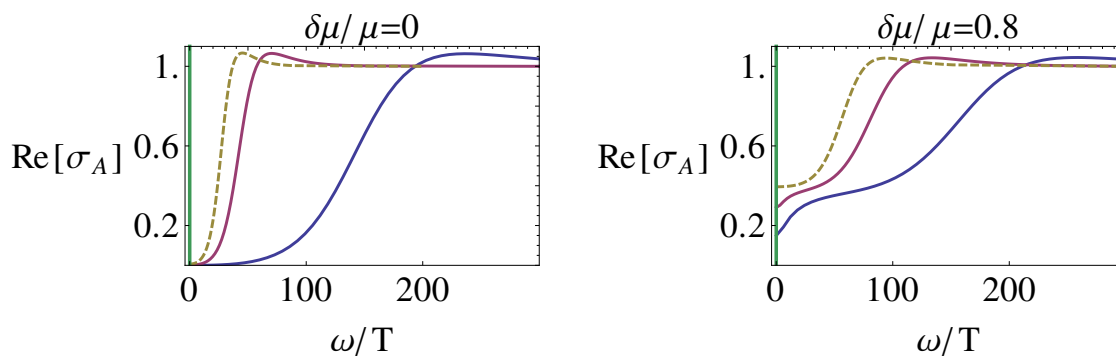


Figure 9. The real part of the electric conductivity for $\delta\mu/\mu = 0, 0.8$ (left plot, right plot) at T_c (dashed curves) and $T < T_c$ (solid curves).

6.4 Conductivities in the superconducting phase

The thermal behavior of the conductivities in the superconducting phase is similar to the one in the normal phase and it is shown in figures 9), (10).

In figures 11), (13, we present the results for $\sigma_A, \sigma_B, \gamma$ in the superconducting phase for $\delta\mu/\mu = 0, 0.8, 1.6$ (dotted, dashed and solid lines respectively) at constant temperature

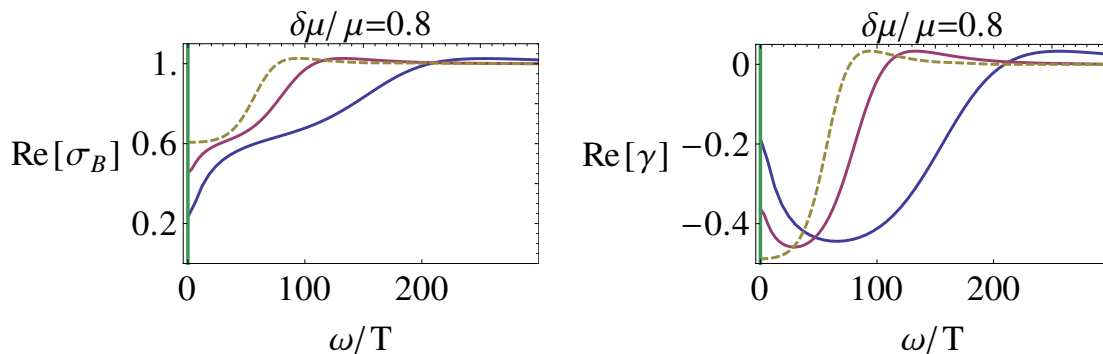


Figure 10. The real part of the “spin-spin conductivity” σ_B (left) and of the “spin conductivity” γ (right) for $\delta\mu/\mu = 0.8$ at T_c (dashed curves) and $T < T_c$ (solid curves).

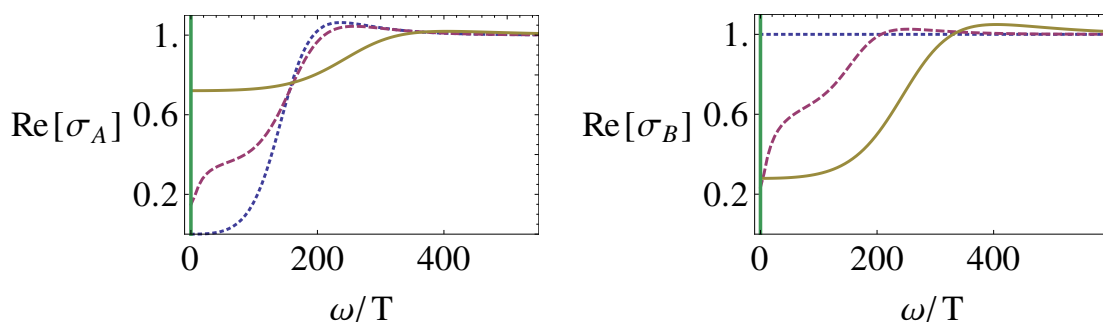


Figure 11. The real part of the electric conductivity σ_A (left) and of the “spin-spin conductivity” σ_B (right) for $\delta\mu/\mu = 0, 0.8, 1.6$ (dotted, dashed and solid lines respectively) at fixed temperature below T_c .

below T_c . The dotted line in figure 11 corresponds to the balanced case ($\delta\mu = 0$) of [27]. The optical electric conductivity at small temperature presents a pseudo-gap²⁴ at small frequencies, while it relaxes to the normal phase value at large ω . The corresponding imaginary part of the conductivity (not shown) has a pole at $\omega = 0$, which translates in a delta function at the same point in $\text{Re}[\sigma_A]$ (the solid line at $\omega/T = 0$ in the figure) due to a Kramers-Kronig relation. A part of this infinite DC conductivity is due to translation invariance and it is present also in the normal phase, as described in section 6.3. Nevertheless, in figure 12 (left plot) it is shown that the imaginary part of the conductivity has discontinuous derivative at T_c , and so the coefficient of the delta function has a jump across the phase transition. This means that a part of the delta function corresponds to genuine superconductivity and is due to the spontaneous breaking of $U(1)_A$ via the condensation of the charged operator dual to ψ .

As $\delta\mu/\mu$ is turned on and increased, the pseudo-gap in the real part of the electric conductivity $\text{Re}[\sigma_A]$ is reduced and eventually lost (dashed and solid lines in figure 11).

²⁴Since the system is really a superfluid, the spectrum is ungapped, containing the Goldstone boson of the breaking of $U(1)_A$. This forbids the presence of a hard gap at $T = 0$ [44]. Nevertheless, the conductivity is extremely small (almost exponentially) at small frequencies for sufficiently low temperatures, hence we speak about a “pseudo-gap”.

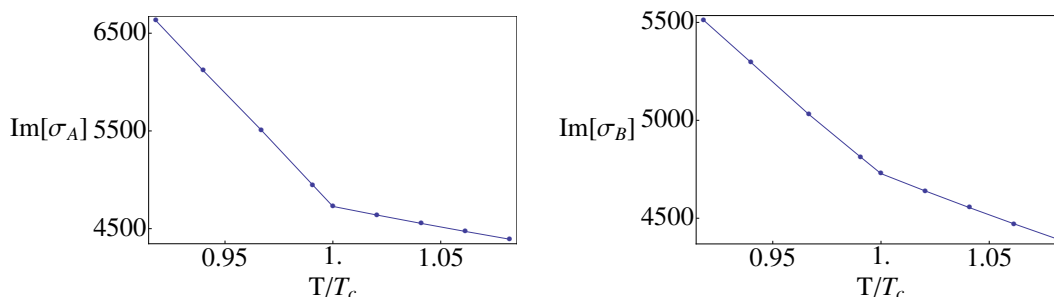


Figure 12. The discontinuity at T_c in the imaginary part of the electric conductivity σ_A (left) and of the “spin-spin conductivity” σ_B (right), signaling a discontinuity in the magnitude of the delta function at $\omega = 0$ in the respective DC conductivities.

This behavior has to be expected, since for large $\delta\mu/\mu$ the system at any fixed temperature will pass, with a second order, continuous transition, to the normal phase; accordingly, the conductivity has a very similar behavior. Precisely the same pattern is seen in the optical conductivities of some iron-based superconductors with increasing doping fraction (e.g. [55]²⁵).

Inversely, from the right plot in figure 11 we see that the real part of the “spin-spin conductivity” $\text{Re}[\sigma_B]$ is more and more depleted at small frequencies as $\delta\mu/\mu$ is increased. Also in this case it can be shown (right plot of figure 12), that the imaginary part of the conductivity has discontinuous derivative at T_c ; the coefficient of the delta function at $\omega = 0$ presents therefore a jump across the phase transition temperature.²⁶ That is, even if the condensing operator is uncharged with respect to $U(1)_B$, due to the mixing with the $U(1)_A$ current in the superconducting phase, the σ_B DC conductivity is enhanced. This strong coupling behavior is in stark contrast with the usual weak coupling picture, where the conductivity σ_B is reduced by the decrease of the quasi-particle population due to the formation of the gap [56].

Figure 13 (left) shows that the “spin conductivity” γ behaves qualitatively as σ_B . For $\delta\mu = 0$ it is constant and vanishing: in absence of “net spin”, an external electric field does not cause the transport of “spin” (and the other way around). Instead, a depletion at small frequencies opens as $\delta\mu/\mu$ is increased and the DC conductivity becomes infinite.

The “current polarization” $P = \text{Re}[J^B]/\text{Re}[J^A]$, measuring the difference of the two DC spin-polarized currents in absence of the “spin motive force”, is exactly equal to $\text{Re}[\gamma]/\text{Re}[\sigma_A]$. In particular, it does not depend on the applied external field E^A . In the normal phase, the relations summarized in (6.26) imply that $P = \delta\rho/\rho$ exactly. In the superconducting phase, it can be checked²⁷ that the qualitative behavior of $P(\delta\rho/\rho)$

²⁵While in Fe-based superconductors the doping dependence does not directly translate into a chemical composition dependence as in cuprates, we chose to mention such an example due to the fact that Fe superconductors are believed to be s-wave (more precisely, s_{+-}), as the ones considered in this paper.

²⁶The existence of this jump can be also verified, following section 4.2 of [27], by considering the analytic form of the small frequency regime of the imaginary part of the conductivity slightly above the critical temperature, and checking numerically that the coefficient of the pole has a discontinuity when going slightly below T_c . The size of this discontinuity is of the same order of the one for σ_A .

²⁷Since the DC conductivities are infinite in the superconducting phase, we estimate the ratio

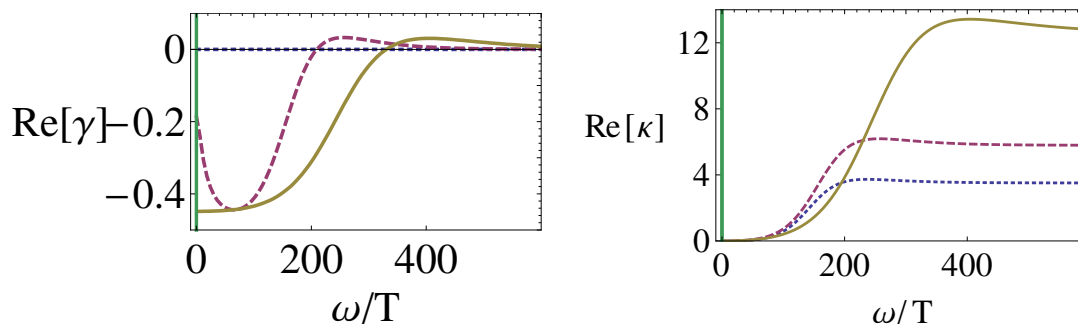


Figure 13. The real part of the “spin conductivity” γ (left) and of the thermal conductivity κ (right) for $\delta\mu/\mu = 0, 0.8, 1.6$ (dotted, dashed and solid lines respectively) at fixed temperature below T_c .

is still increasing, but in a non-linear way (the power dependence being larger than one). For examples of current polarization behaviors in BCS systems, see e.g. [57]. The “optical current polarization”, instead, can be shown to be non-monotonic with $\delta\rho/\rho$.

In the presence of the condensate, the symmetries encountered in the normal phase and encoded in formulas (6.24), (6.26) are explicitly broken (relations (6.20), (6.21) and (6.23) are preserved). In particular, (6.26) should be modified to account for the vev of the charged operator, which heavily influences the small frequency behavior of the conductivities. Unfortunately, we did not find any simple modification that accounts for the numerical results.

At this point, a comment is in order. It is clear that for non-extremal values of $\delta\mu/\mu$, exemplified by the dashed lines in the figures of this section, the conductivities have a non-trivial (even non-monotonic) behavior for small frequencies.²⁸ This is reasonable. In fact, the presence of the new energy scale provided by the imbalance can modify, with respect to the balanced case, the behavior of the system at frequencies related to $\delta\mu$. We know from [53] that the behavior of the balanced system at zero charge density has just one regime at zero momentum: the hydrodynamic and the high frequency regimes coincide and the conductivity is constant. On the other hand, the condensate in the charged system changes drastically the behavior of the electric conductivity in the small frequency regime, which is now dominated by the superfluid Goldstone mode and the pseudo-gap [26, 44]. It is thus natural to expect a non-trivial influence of the extra IR scale $\delta\mu$ on the transport properties of the theory. In particular, from the plots of this section it seems that the DC electric conductivity is further enhanced by $\delta\mu$ w.r.t. the extrapolated behavior of the normal phase, possibly due to a second light mode.

The thermo-electric, “spin-electric” and thermal conductivity follow from the plots above and formulas (6.20), (6.21), (6.23). The corresponding plots are reported in figure 13 (right) and 14.

$\text{Re}[\gamma]/\text{Re}[\sigma_A]$ by evaluating the corresponding ratio of imaginary parts at very small ω/T , relying on the Kramers-Kronig relation for the result to translate in the respective behavior of the real parts.

²⁸We think that this behavior is not due to numerical effects because we checked it with two independent codes and two different methods for the calculations.

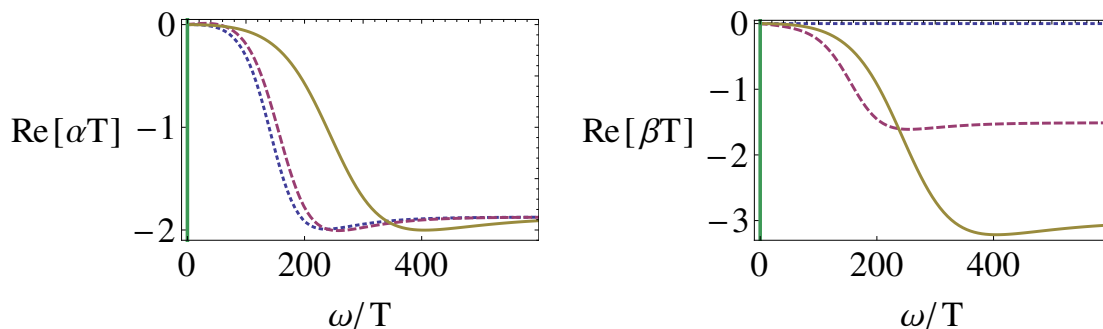


Figure 14. The real part of the thermo-electric and “thermo-spin” conductivities (left plot, right plot) for $\delta\mu/\mu = 0, 0.8, 1.6$ (dotted, dashed and solid lines respectively) at fixed temperature below T_c .

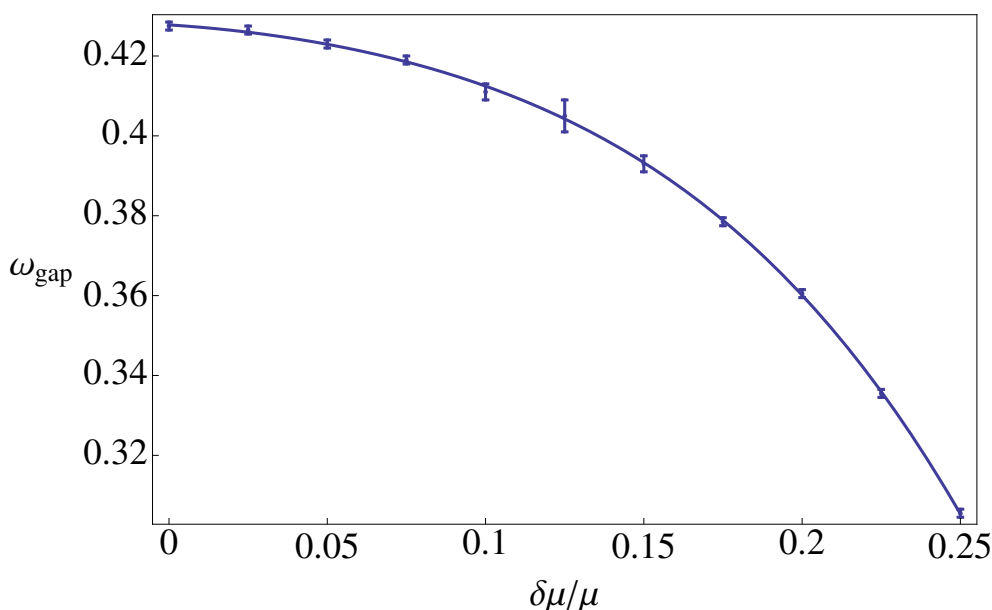


Figure 15. The “pseudo-gap” frequency ω_{gap} as a function of $\delta\mu/\mu$ at fixed T . The error bars are associated to numerical uncertainty and the plotted line emerges from a fit with a quartic polynomial.

Finally, in figure 15 we report the plot of the “pseudo-gap” frequency ω_{gap} below which the real part of the optical electric conductivity σ_A is essentially vanishing,²⁹ at constant temperature but increasing $\delta\mu/\mu$. The behavior of $\omega_{\text{gap}}(\delta\mu/\mu)$ is clearly non-linearly decreasing. This has to be compared to the case of ordinary unbalanced superconductors, where the gap Δ is constant in $\delta\mu$ at $T = 0$. In [27] it was pointed out that $\omega_{\text{gap}}(\delta\mu = 0)/T_c^0 \sim 8$ as in some measures in high T_c superconductors. We find that $\omega_{\text{gap}}(\delta\mu/\mu)/T_c$ is not approximately constant, but a decreasing function of $\delta\mu/\mu$ which substantially deviates from the value 8 even in the range of $\delta\mu/\mu$ where it is still reasonably well defined.

²⁹To be precise, we used the numerical threshold value $\text{Re}[\sigma_A(\omega_{\text{gap}})] = 0.005$.

7 Comments on possible string embeddings

If the results we have found on “charge” and “spin” transport properties have some degree of universality, as we have argued above, the same is not necessarily true for equilibrium properties. The $(T, \delta\mu)$ phase diagram, for example, can vary for different choices of the scalar potential, as it happens in the balanced case (see for example [58–60]). This variation accounts for different microscopic properties of the dual field theories which are however unknown. The latter could be unveiled only by embedding the bottom-up models in full-fledged string or M-theory constructions.

The embeddings depend both on the spacetime dimensionality and on the microscopical details of the dual field theory — essentially on the kind of $U(1)$ gauge fields entering the game and on the precise nature of the order parameter. The latter can in fact be a condensate of, say, adjoint (or more generic two-index representations of some gauge group) or fundamental fermionic degrees of freedom and the string or M-theory embedding would strongly depend on whether one or another possibility is realized.

7.1 Adjoint fermion condensates

In supersymmetric contexts, this is a case where, say, gluino bilinears break some $U(1)_R$ symmetry of the theory.³⁰ In this case we should try to see whether our minimal $3 + 1$ dimensional gravity model can arise from a consistent Kaluza-Klein truncation of 11d-supergravity on some compact seven-manifold, in the same way as it happens (see [62–65]) for the balanced model introduced in [26]. Isometries of the seven-manifold, in fact, are mapped into global (R-) symmetries of the dual field theory. At least within known consistent KK truncations (see e.g. [63–65]) it seems that an embedding of a fully backreacted model containing the same fields as ours is possible only provided at least another non-trivial real scalar field is present. This is true also in the normal phase, i.e. in the absence of our complex scalar field.

To see this explicitly, let us consider the KK reduction of 11d-supergravity on a seven sphere S^7 . This gives rise to gauged $d = 4$, $\mathcal{N} = 8$ $SO(8)$ supergravity, which can be further truncated to a gauged $\mathcal{N} = 2$ model where the bosonic sector consists of the metric, four Maxwell fields A_μ^A , three “dilaton” ϕ_i and three “axions” [66]. The resulting Lagrangian density reads

$$(\sqrt{\det g})^{-1} \mathcal{L} = R - \frac{1}{2} \sum_{i=1}^3 [(\partial\phi_i)^2 + 8g^2(\cosh\phi_i)] - \frac{1}{4} \sum_{A=1}^4 \sum_{i=1}^3 e^{a^i_A \phi_i} (F^A)^2 + \dots, \quad (7.1)$$

where g is the coupling, a^i_A are constants and we have not included the contribution of the axions. This action cannot be further truncated to a model with constant dilatons and two *independent* non-trivial Maxwell fields. Such kind of truncation is only allowed if the $U(1)$ fields are identified up to some constant (hence in the balanced case), and this constraint applies also to more general KK truncations [63–65].

³⁰ $U(1)_R$ superfluidity driven by gluino Cooper pairs in $\mathcal{N} = 4$ SYM at finite density has been first considered in [61].

The same conclusion holds in the $d = 5$ case, i.e. considering abelian [66] or non-abelian gauged supergravities [67] obtained from consistent KK truncations of IIB supergravity. For example in the first reference in [63–65] it is shown how a $U(1)^2$ -charged RN-AdS black hole solution like the one describing the normal phase in our model, can be embedded within Romans’ $\mathcal{N} = 4$ $SU(2) \times U(1)$ gauged supergravity [67] (and thus in type IIB), only if the two Maxwell fields (and so the corresponding chemical potentials) are identified modulo a constant. Again, a setup where the two fields are independent can only be realized adding a non-trivial real scalar (dilaton-like) field. Embeddings of balanced superconductors [68], instead, do not require this extra scalar to be present.

7.2 Fundamental fermion condensates

³¹ Matter fields transforming in the fundamental representation are introduced in the holographic correspondence by means of flavor D-branes. Models of holographic p-wave superconductivity have been actually embedded in probe flavor brane setups [28, 69, 70]. Here we want to focus on the s-wave case. Having in mind 4d QCD-like models, one could consider, say, a non-critical 5d string model with N_c D3 and N_f spacetime filling D4-anti-D4 branes [71, 72]. The low-energy modes of the D3-branes would be the $SU(N_c)$ gluons, and the D4-anti-D4 branes would provide the left and right handed fundamental flavor fields (the quarks). The model contains a complex scalar field (the would-be tachyon of the open string stretching between branes and anti-branes) transforming in the (anti)fundamental of $SU(N_f)_L \times SU(N_f)_R$: its condensation (eventually triggered by a running dilaton which can account for confinement) drives the breaking of the chiral symmetry down to $SU(N_f)$ and thus it is dual to the chiral condensate of fundamental fermions [71–73]. The model (at least a simplified version of it [71]) can provide AdS_5 flavored solutions (at zero temperature and densities) with trivial tachyon and constant dilaton. These are possibly dual to phases of the theory in Banks-Zacks-like conformal windows. The corresponding finite temperature versions have been studied in [74, 75].

Let us start considering the $N_f = 1$ case. In addition to the above mentioned complex scalar field τ , the DBI brane-antibrane action [76–78] contains two Maxwell fields and it is coupled with the dilaton. The scalar field τ is charged under a combination of the two gauge fields (the “chiral” $U(1)_A$) and uncharged under the orthogonal combination (the “baryonic” $U(1)_B$). The chiral symmetry is actually anomalous and this is accounted for by other terms in the D-brane action [72]. One can consider $N_f > 1$ setups, e.g. $N_f = 2$ ones, enhancing the preserved flavor symmetry to an $SU(2) \times U(1)_B$ one. Starting from the above mentioned flavored-AdS solutions one could turn on a chemical potential for a $U(1)_I \subset SU(N_f)$ “isospin” field as well as a baryonic one. Analogously to our condensed matter setup, one could then study the stability of the system under fluctuations of the complex scalar field τ . The latter would be dual to, say, a $\bar{u}d$ mesonic condensate and thus the role of $\delta\mu$ and μ would be played by μ_B and μ_I respectively. Let us focus on the $N_f = 1$ case for simplicity, treating the axial $U(1)_A$ as if it would be a genuine symmetry replacing $U(1)_I$, i.e. neglecting all the terms in the brane action which are related to its anomaly.

³¹We are grateful to Emiliano Imeroni for his contributions to this part of the project.

The Dp -brane-anti-brane DBI action in string frame reads [76–78]

$$S = -T_p \int d^{p+1}x e^{-\Phi} V(|\tau|) \left[\sqrt{-\det \mathbf{A}^{(L)}} + \sqrt{-\det \mathbf{A}^{(R)}} \right], \quad (7.2)$$

where T_p is the D-brane tension, Φ is the dilaton and $V(|\tau|)$ is the open string tachyon potential. Let us assume that a closed string tachyon, which could be present in non-critical Type 0 setups, is eventually frozen out. The matrices $\mathbf{A}^{(L),(R)}$ in (7.2) are defined as

$$\begin{aligned} \mathbf{A}_{MN}^{(i)} &= P[g + B_2]_{MN} + 2\pi\alpha' F_{MN}^{(i)} + \pi\alpha' (D_M\tau)^* (D_N\tau) + \pi\alpha' (D_N\tau)^* (D_M\tau), \\ F_{MN}^{(i)} &= \partial_M A_N^{(i)} - \partial_N A_M^{(i)}, \\ D_M\tau &= (\partial_M + iA_M^{(L)} - iA_M^{(R)})\tau, \end{aligned} \quad (7.3)$$

where $i = L, R$ label the brane or antibrane, $P[\bullet]$ denotes the pullback on the D-brane worldvolume, g is the metric and B_2 is the NSNS antisymmetric two-form. Notice that, as anticipated, the scalar field is charged only under the axial $U(1)_A$ combination

$$A_M = A_M^{(L)} - A_M^{(R)}. \quad (7.4)$$

It is instead uncharged under the barionic $U(1)_B$ combination

$$B_M = A_M^{(L)} + A_M^{(R)}. \quad (7.5)$$

In the case of brane-antibrane pairs in flat spacetime, string field theory gives a tachyon potential of the form

$$V(|\tau|) = e^{\pi\alpha' m^2 |\tau|^2}, \quad \text{with } m^2 = -\frac{1}{2\alpha'}. \quad (7.6)$$

This expression could be affected by non-trivial field redefinitions and by the fact that the branes have to be put on curved spacetimes (see e.g. a discussion in [72]). Anyway, we will take this expression as a guideline.

As for the embedding described in the previous subsection, when independent Maxwell fields are both turned on, it seems not possible to have solutions with non-trivial dilaton (it is understood that the whole gravity action, say for $p = 4$, will be a “bulk+brane” one with the standard kinetic term for the dilaton). Notice that in the model the Maxwell fields are coupled by the non-linear structure of the DBI action and thus spintronics effects could be present also in the non-fully backreacted case.

Let us just notice, finally, that on a closed string background where $B_2 = 0$ and the metric is diagonal, the low energy effective Lagrangian density coming from (7.2) at the quadratic level in the fields is (see eq. (10) in the second paper in [77, 78] and use our redefinitions (7.4), (7.5))

$$\mathcal{L} \approx -T_p (2\pi\alpha') e^{-\Phi} \sqrt{g} \left[-\pi\alpha' F^2 - \pi\alpha' Y^2 + |D\tau|^2 + m^2 |\tau|^2 \right], \quad (7.7)$$

where $F = dA$, $Y = dB$ and $D\tau = (\partial - iA)\tau$. This has, modulo coefficients and the overall dilaton coupling, the same form as the matter part of our gravity model.

Acknowledgments

We are very grateful to Emiliano Imeroni for his collaboration in the initial stages of this work and to Matteo Bertolini, Pasquale Calabrese, Andrea Cappelli, Roberto Casalbuoni, Davide Forcella, Iroshi Kohno, Alberto Lerda, Massimo Mannarelli, Alberto Mariotti, Mikhail Mintchev, Giovanni Ummarino and Paola Verrucchi for many relevant comments, advices, discussions and E-mail correspondence. This work was supported in part by the MIUR-PRIN contract 2009-KHZKRX. The research of A. L. C. and F. B. is supported by the European Community Seventh Framework Programme FP7/2007-2013, under grant agreements n. 253534 and 253937.

We would like to thank the Italian students, parents, teachers and scientists for their activity in support of public education and research.

A The Chandrasekhar-Clogston bound

Let us consider a Fermi mixture with two species u and d (e.g. dressed electrons of spin up and down in metallic superconductors) with different chemical potentials μ_u and μ_d . Let us define the mean chemical potential μ and the chemical potential imbalance $\delta\mu$ as

$$\mu = \frac{1}{2}(\mu_u + \mu_d) \quad \delta\mu = \frac{1}{2}(\mu_u - \mu_d). \quad (\text{A.1})$$

Assuming analyticity, in the grand-canonical ensemble, the Gibbs free energy $\Omega(\delta\mu)$ at zero temperature can be Taylor expanded for $\delta\mu \ll \mu$ as

$$\Omega(\delta\mu) = \Omega(0) + \Omega(0)' \delta\mu + \frac{1}{2} \Omega''(0) \delta\mu^2 + \mathcal{O}(\delta\mu^3). \quad (\text{A.2})$$

The first (resp. second) derivative of Ω w.r.t. $\delta\mu$ defines the population imbalance δn (resp. the susceptibility imbalance³² $\delta\chi$)

$$\delta n \equiv n_u - n_d = -\frac{\partial \Omega}{\partial \delta\mu}, \quad \delta\chi = \frac{\partial \delta n}{\partial \delta\mu} = -\frac{\partial^2 \Omega}{\partial \delta\mu^2}. \quad (\text{A.3})$$

In BCS theory, the normal phase at $T = 0$ and $\delta\mu \ll \mu$ has a population imbalance given by $\delta n_N \approx \rho_F \delta\mu$, where ρ_F is the two-Fermion density of states at the mean Fermi surface $E = E_F = \mu$. From this expression we easily find that, in the normal phase, the free energy expansion (A.2) reduces at leading order to

$$\Omega_N(\delta\mu) \approx \Omega_N(0) - \frac{1}{2} \rho_F \delta\mu^2. \quad (\text{A.4})$$

At $T = 0$, the homogeneous BCS superconducting phase, characterized by Cooper pairs of zero total momentum, has an equal number of particles of species 1 and 2: $\delta n_S = 0$. Thus the free energy just expands as

$$\Omega_S(\delta\mu) \approx \Omega_S(0). \quad (\text{A.5})$$

³²In the case where the chemical potential imbalance is induced by the Zeeman coupling with a magnetic field, this is actually the magnetic susceptibility.

The difference between the two free energies is given by

$$\Omega_N(\delta\mu) - \Omega_S(\delta\mu) \approx \Omega_N(0) - \Omega_S(0) - \frac{1}{2}\rho_F\delta\mu^2. \quad (\text{A.6})$$

Now, using the standard BCS result, $\Omega_N(0) - \Omega_S(0) = \rho_F\Delta_0^2/4$, where Δ_0 is the gap parameter at $T = 0$, it follows that

$$\Omega_N(\delta\mu) - \Omega_S(\delta\mu) \approx \frac{1}{4}\rho_F\Delta_0^2 - \frac{1}{2}\rho_F\delta\mu^2. \quad (\text{A.7})$$

This shows that at $T = 0$ the superconducting phase is favored (i.e. its free energy is less than the free energy of the normal phase) only if the Chandrasekhar-Clogston bound

$$\delta\mu < \delta\mu_1, \quad \delta\mu_1 \equiv \frac{\Delta_0}{\sqrt{2}}, \quad (\text{A.8})$$

is satisfied.

B Equations of motion in $d + 1$ bulk spacetime dimensions

Let us consider the generalization of our model to $d + 1$ -dimensions. The action reads

$$S = \frac{1}{2k_{d+1}^2} \int dx^{d+1} \sqrt{-g} \left[\mathcal{R} + \frac{d(d-1)}{L^2} - \frac{1}{4}F_{ab}F^{ab} - \frac{1}{4}Y_{ab}Y^{ab} - V(|\psi|) - |\partial\psi - iqA\psi|^2 \right]. \quad (\text{B.1})$$

The ansatz for the spacetime metric is

$$ds^2 = -g(r)e^{-\chi(r)}dt^2 + \frac{r^2}{L^2}d\vec{x}^2 + \frac{dr^2}{g(r)}, \quad (\text{B.2})$$

together with an homogeneous ansatz for the fields

$$\psi = \psi(r), \quad A_a dx^a = \phi(r)dt, \quad B_a dx^a = v(r)dt. \quad (\text{B.3})$$

The equation of motion for the scalar field reads

$$\psi'' + \psi' \left(\frac{g'}{g} + \frac{(d-1)}{r} - \frac{\chi'}{2} \right) - \frac{1}{2} \frac{V'(\psi)}{g} + \frac{e^\chi q^2 \phi^2 \psi}{g^2} = 0. \quad (\text{B.4})$$

Maxwell's equation for the ϕ field gives

$$\phi'' + \phi' \left(\frac{(d-1)}{r} + \frac{\chi'}{2} \right) - 2 \frac{q^2 \phi \psi^2}{g} = 0. \quad (\text{B.5})$$

Einstein's equations reduce to

$$\begin{aligned} \frac{1}{2}\psi'^2 + \frac{e^\chi(\phi'^2 + v'^2)}{4g} + \frac{(d-1)}{2} \frac{g'}{gr} \\ + \frac{1}{2} \frac{(d-1)(d-2)}{r^2} - \frac{d(d-1)}{2gL^2} + \frac{V(\psi)}{2g} + \frac{q^2\psi^2\phi^2 e^\chi}{2g^2} = 0, \\ \chi' + \frac{2}{(d-1)} r\psi'^2 + \frac{2}{(d-1)} r \frac{q^2\phi^2\psi^2 e^\chi}{g^2} = 0. \end{aligned} \quad (\text{B.6})$$

Finally, Maxwell's equations for the additional gauge field read

$$v'' + v' \left(\frac{(d-1)}{r} + \frac{\chi'}{2} \right) = 0. \quad (\text{B.7})$$

B.1 The normal phase

The gravity solution corresponding to the normal phase in the dual d -dimensional field theory is the $U(1)^2$ - charged Reissner-Nördstrom (RN)- AdS_{d+1} black hole

$$ds^2 = -g(r)dt^2 + \frac{r^2}{L^2}d\vec{x}^2 + \frac{dr^2}{g(r)}, \quad (\text{B.8})$$

$$g(r) = \frac{r^2}{L^2} \left(1 - \frac{r_H^d}{r^d}\right) + \frac{1}{2} \frac{(d-2)}{(d-1)} (\mu^2 + \delta\mu^2) \left(\frac{r_H}{r}\right)^{2(d-2)} \left(1 - \left(\frac{r}{r_H}\right)^{d-2}\right), \quad (\text{B.9})$$

$$A_t = \mu \left(1 - \left(\frac{r_H}{r}\right)^{d-2}\right), \quad (\text{B.10})$$

$$B_t = \delta\mu \left(1 - \left(\frac{r_H}{r}\right)^{d-2}\right), \quad (\text{B.11})$$

where $r = r_H$ is the position of the outer horizon.

The charge densities of the dual field theory are related to the subleading behavior of the bulk Maxwell fields as

$$\rho = \frac{1}{2k_{d+1}^2} \frac{(d-2)\mu r_H^{d-2}}{L^{d-1}}, \quad \delta\rho = \frac{1}{2k_{d+1}^2} \frac{(d-2)\delta\mu r_H^{d-2}}{L^{d-1}}. \quad (\text{B.12})$$

The black hole temperature is

$$T = \frac{r_H}{4\pi L^2} \left[d - \frac{(d-2)^2}{(d-1)} \frac{(\mu^2 + \delta\mu^2)L^2}{2r_H^2} \right]. \quad (\text{B.13})$$

The Gibbs free energy density (hence the pressure) is given by

$$\omega = -p = -\frac{1}{2k_{d+1}^2} \frac{r_H^d}{L^{d+1}} \left(1 + \frac{(d-2)}{2(d-1)} \frac{(\mu^2 + \delta\mu^2)L^2}{r_H^2}\right). \quad (\text{B.14})$$

Consistently, the charge densities in (B.12) are obtained as

$$\rho = -\frac{\partial\omega}{\partial\mu}, \quad \delta\rho = -\frac{\partial\omega}{\partial\delta\mu}. \quad (\text{B.15})$$

The energy density is given by

$$\epsilon = \frac{d-1}{k_{d+1}^2} \frac{r_H^d}{L^{d+1}} \left(1 + \frac{(d-2)}{2(d-1)} \frac{(\mu^2 + \delta\mu^2)L^2}{r_H^2}\right). \quad (\text{B.16})$$

This satisfies the relation $\epsilon = (d-1)p$ related to the vanishing of the trace of the stress energy tensor.

B.1.1 Near horizon geometry

The Reissner-Nordstrom geometry is interesting as $T \rightarrow 0$. In this limit the horizon radius has a fixed value at

$$r_H^2 = \frac{1}{2d} \frac{(d-2)^2 L^2 \mu^2}{(d-1)}. \quad (\text{B.17})$$

To find the near horizon metric take the series Taylor expansion of the blackening factor

$$g(r) \simeq g(r_H) + g'(r_H)\tilde{r} + \frac{1}{2}g''(r_H)\tilde{r}^2, \quad (\text{B.18})$$

where again $r = r_H + \tilde{r}$ with $\tilde{r} \rightarrow 0$. We find that

$$g(r_H) = 0, \quad g'(r_H) \sim T = 0, \quad g''(r_H) = \frac{2d(d-1)}{L^2}. \quad (\text{B.19})$$

The near horizon metric reads then

$$ds_{\text{near horizon}}^2 \simeq -d(d-1)\frac{\tilde{r}^2}{L^2}dt^2 + \frac{r_H^2}{L^2}d\vec{x}^2 + \frac{L^2}{d(d-1)\tilde{r}^2}d\tilde{r}^2, \quad (\text{B.20})$$

from which we recognize the $AdS_2 \times R^{d-1}$ metric. The AdS_2 radius squared is $L_{(2)}^2 = L^2/(d(d-1))$.

B.2 Criterion for instability

Let us consider the stability of the above solution at $T = 0$ under fluctuations of the charged scalar field. The equation one has to consider is given in (B.4). The background is the extremal doubly charged RN- AdS_{d+1} . In the near horizon limit it is easy to show that the equation of motion for ψ reduces to that of a scalar field of effective mass

$$m_{(2)}^2 = m^2 - \frac{2q^2}{1+x^2}, \quad x \equiv \delta\mu/\mu, \quad (\text{B.21})$$

on an AdS_2 background of radius $L_{(2)}^2 = L^2/(d(d-1))$.

The background is unstable in the limit if the BF bound in AdS_2 is violated, i.e. if $L_{(2)}^2 m_{(2)}^2 < -1/4$. This is equivalent to the condition

$$\left(1 + \frac{\delta\mu^2}{\mu^2}\right) \left(m^2 + \frac{d(d-1)}{4}\right) < 2q^2, \quad (\text{B.22})$$

which generalizes our formula (4.14) valid for $d = 3$.

Open Access. This article is distributed under the terms of the Creative Commons Attribution License which permits any use, distribution and reproduction in any medium, provided the original author(s) and source are credited.

References

- [1] R. Casalbuoni and G. Nardulli, *Inhomogeneous superconductivity in condensed matter and QCD*, *Rev. Mod. Phys.* **76** (2004) 263 [[hep-ph/0305069](#)] [[INSPIRE](#)].
- [2] A. Iarkin and Y. Ovchinnikov, *Nonuniform state of superconductors*, *Zh. Eksp. Teor. Fiz.* **47** (1964) 1136 [[INSPIRE](#)].
- [3] P. Fulde and R.A. Ferrell, *Superconductivity in a strong spin-exchange field*, *Phys. Rev.* **135** (1964) A 550 [[INSPIRE](#)].

- [4] B.S. Chandrasekhar, *A note on the maximum critical field of high field superconductors*, *Appl. Phys. Lett.* **1** (1962) 7.
- [5] A.M. Clogston, *Upper limit for the critical field in hard superconductors*, *Phys. Rev. Lett.* **9** (1962) 266.
- [6] A. Fert, *Nobel lecture: origin, development and future of spintronics*, *Rev. Mod. Phys.* **80** (2008) 1517 [INSPIRE].
- [7] I. Zutic, J. Fabian and S. Das Sarma, *Spintronics: fundamentals and applications*, *Rev. Mod. Phys.* **76** (2004) 1323.
- [8] N.F. Mott, *The electrical conductivity of transition metals*, *Proc. Roy. Soc. Lond. A* **153** (1936) 699.
- [9] N.F. Mott, *The resistance and thermoelectric properties of the transition metals*, *Proc. Roy. Soc. Lond. A* **156** (1936) 368.
- [10] A. Fert and I.A. Campbell, *Two-current conduction in nickel*, *Phys. Rev. Lett.* **21** (1968) 1190.
- [11] P.C. van Son, H. van Kempen and P. Wyder, *Boundary resistance of the ferromagnetic-nonferromagnetic metal interface*, *Phys. Rev. Lett.* **58** (1987) 2271.
- [12] M. Johnson and R. H. Silsbee, *Thermodynamic analysis of interfacial transport and of the thermomagnetolectric system*, *Phys. Rev. B* **35** (1987) 4959.
- [13] N. Iqbal, H. Liu, M. Mezei and Q. Si, *Quantum phase transitions in holographic models of magnetism and superconductors*, *Phys. Rev. D* **82** (2010) 045002 [arXiv:1003.0010] [INSPIRE].
- [14] K.W. Kim, J.W. Moon and K.J. Lee, *Effect of spin diffusion on current generated by spin motive force*, *Phys. Rev. B* **84** (2011) 054462.
- [15] J. Shibata and H. Kohno, *Spin and charge transport induced by gauge fields in a ferromagnet*, *Phys. Rev. B* **84** (2011) 184408 [arXiv:1107.2165].
- [16] S.A. Hartnoll, *Lectures on holographic methods for condensed matter physics*, *Class. Quant. Grav.* **26** (2009) 224002 [arXiv:0903.3246] [INSPIRE].
- [17] C.P. Herzog, *Lectures on holographic superfluidity and superconductivity*, *J. Phys. A* **42** (2009) 343001 [arXiv:0904.1975] [INSPIRE].
- [18] S.-J. Rey, *String theory on thin semiconductors: holographic realization of Fermi points and surfaces*, *Prog. Theor. Phys. Suppl.* **177** (2009) 128 [arXiv:0911.5295] [INSPIRE].
- [19] G.T. Horowitz, *Introduction to holographic superconductors*, arXiv:1002.1722 [INSPIRE].
- [20] S.A. Hartnoll, *Horizons, holography and condensed matter*, arXiv:1106.4324 [INSPIRE].
- [21] S. Sachdev, *What can gauge-gravity duality teach us about condensed matter physics?*, arXiv:1108.1197 [INSPIRE].
- [22] N. Iqbal, H. Liu and M. Mezei, *Lectures on holographic non-Fermi liquids and quantum phase transitions*, arXiv:1110.3814 [INSPIRE].
- [23] S. Sachdev, *Condensed matter and AdS/CFT*, arXiv:1002.2947 [INSPIRE].
- [24] S. Sachdev and B. Keimer, *Quantum criticality*, *Phys. Today* **64N2** (2011) 29 [arXiv:1102.4628].

- [25] S.S. Gubser, *Breaking an abelian gauge symmetry near a black hole horizon*, *Phys. Rev. D* **78** (2008) 065034 [[arXiv:0801.2977](#)] [[INSPIRE](#)].
- [26] S.A. Hartnoll, C.P. Herzog and G.T. Horowitz, *Building a holographic superconductor*, *Phys. Rev. Lett.* **101** (2008) 031601 [[arXiv:0803.3295](#)] [[INSPIRE](#)].
- [27] S.A. Hartnoll, C.P. Herzog and G.T. Horowitz, *Holographic superconductors*, *JHEP* **12** (2008) 015 [[arXiv:0810.1563](#)] [[INSPIRE](#)].
- [28] J. Erdmenger, V. Grass, P. Kerner and T.H. Ngo, *Holographic superfluidity in imbalanced Mixtures*, *JHEP* **08** (2011) 037 [[arXiv:1103.4145](#)] [[INSPIRE](#)].
- [29] S.S. Gubser, *Colorful horizons with charge in Anti-de Sitter space*, *Phys. Rev. Lett.* **101** (2008) 191601 [[arXiv:0803.3483](#)] [[INSPIRE](#)].
- [30] S.S. Gubser and S.S. Pufu, *The gravity dual of a p-wave superconductor*, *JHEP* **11** (2008) 033 [[arXiv:0805.2960](#)] [[INSPIRE](#)].
- [31] A. Donos and J.P. Gauntlett, *Holographic striped phases*, *JHEP* **08** (2011) 140 [[arXiv:1106.2004](#)] [[INSPIRE](#)].
- [32] A. Donos, J.P. Gauntlett and C. Pantelidou, *Spatially modulated instabilities of magnetic black branes*, *JHEP* **01** (2012) 061 [[arXiv:1109.0471](#)] [[INSPIRE](#)].
- [33] A. Donos and J.P. Gauntlett, *Holographic helical superconductors*, *JHEP* **12** (2011) 091 [[arXiv:1109.3866](#)] [[INSPIRE](#)].
- [34] R. Combescot, *Introduction to FFLO phases and collective mode in the BEC-BCS crossover*, [cond-mat/0702399](#).
- [35] R. Combescot and C. Mora, *Transition to Fulde-Ferrel-Larkin-Ovchinnikov phases near the tricritical point: an analytical study*, *Eur. Phys. J. B* **28** (2002) 397 [[cond-mat/0203031](#)].
- [36] M.G. Alford, K. Rajagopal and F. Wilczek, *Color flavor locking and chiral symmetry breaking in high density QCD*, *Nucl. Phys. B* **537** (1999) 443 [[hep-ph/9804403](#)] [[INSPIRE](#)].
- [37] K. Rajagopal and F. Wilczek, *The condensed matter physics of QCD*, in *At the frontier of particle physics, volume 3*, M. Shifman ed., World Scientific, Singapore (2001), [hep-ph/0011333](#) [[INSPIRE](#)].
- [38] M.G. Alford, A. Schmitt, K. Rajagopal and T. Schafer, *Color superconductivity in dense quark matter*, *Rev. Mod. Phys.* **80** (2008) 1455 [[arXiv:0709.4635](#)] [[INSPIRE](#)].
- [39] M. Alford, J.A. Bowers and K. Rajagopal, *Crystalline color superconductivity*, *Phys. Rev. D* **63** (2001) 074016 [[hep-ph/0008208](#)] [[INSPIRE](#)].
- [40] S. Giorgini, L.P. Pitaevskii and S. Stringari, *Theory of ultracold atomic Fermi gases*, *Rev. Mod. Phys.* **80** (2008) 1215 [[arXiv:0706.3360](#)] [[INSPIRE](#)].
- [41] M.W. Zwierlein, A. Schirotzek, C.H. Schunck and W. Ketterle, *Fermionic superfluidity with imbalanced spin populations*, *Science* **311** (2006) 492 [[INSPIRE](#)].
- [42] P.F. Bedaque, H. Caldas and G. Rupak, *Phase separation in asymmetrical fermion superfluids*, *Phys. Rev. Lett.* **91** (2003) 247002 [[cond-mat/0306694](#)] [[INSPIRE](#)].
- [43] M. Mannarelli, G. Nardulli and M. Ruggieri, *Evaluating the phase diagram of superconductors with asymmetric spin populations*, *Phys. Rev. A* **74** (2006) 033606 [[cond-mat/0604579](#)] [[INSPIRE](#)].

- [44] G.T. Horowitz and M.M. Roberts, *Zero temperature limit of holographic superconductors*, *JHEP* **11** (2009) 015 [[arXiv:0908.3677](#)] [[INSPIRE](#)].
- [45] D.B. Kaplan, J.-W. Lee, D.T. Son and M.A. Stephanov, *Conformality lost*, *Phys. Rev. D* **80** (2009) 125005 [[arXiv:0905.4752](#)] [[INSPIRE](#)].
- [46] K. Jensen, A. Karch, D.T. Son and E.G. Thompson, *Holographic Berezinskii-Kosterlitz-Thouless transitions*, *Phys. Rev. Lett.* **105** (2010) 041601 [[arXiv:1002.3159](#)] [[INSPIRE](#)].
- [47] E. Nakano and W.-Y. Wen, *Critical magnetic field in a holographic superconductor*, *Phys. Rev. D* **78** (2008) 046004 [[arXiv:0804.3180](#)] [[INSPIRE](#)].
- [48] S. Nakamura, H. Ooguri and C.-S. Park, *Gravity dual of spatially modulated phase*, *Phys. Rev. D* **81** (2010) 044018 [[arXiv:0911.0679](#)] [[INSPIRE](#)].
- [49] P. Basu, A. Mukherjee and H.-H. Shieh, *Supercurrent: vector hair for an AdS black hole*, *Phys. Rev. D* **79** (2009) 045010 [[arXiv:0809.4494](#)] [[INSPIRE](#)].
- [50] C. Herzog, P. Kovtun and D. Son, *Holographic model of superfluidity*, *Phys. Rev. D* **79** (2009) 066002 [[arXiv:0809.4870](#)] [[INSPIRE](#)].
- [51] D. Arean, P. Basu and C. Krishnan, *The many phases of holographic superfluids*, *JHEP* **10** (2010) 006 [[arXiv:1006.5165](#)] [[INSPIRE](#)].
- [52] D. Arean, M. Bertolini, C. Krishnan and T. Prochazka, *Quantum critical superfluid flows and anisotropic domain walls*, *JHEP* **09** (2011) 131 [[arXiv:1106.1053](#)] [[INSPIRE](#)].
- [53] C.P. Herzog, P. Kovtun, S. Sachdev and D.T. Son, *Quantum critical transport, duality and M-theory*, *Phys. Rev. D* **75** (2007) 085020 [[hep-th/0701036](#)] [[INSPIRE](#)].
- [54] B. Bellazzini, M. Burrello, M. Mintchev and P. Sorba, *Quantum field theory on star graphs*, *Proc. Symp. Pure Math.* **77** (2008) 639 [[arXiv:0801.2852](#)] [[INSPIRE](#)].
- [55] M. Nakajima et al., *Evolution of the optical spectrum with doping in $Ba(Fe_{1-x}Co_x)_2As_2$* , *Phys. Rev. B* **81** (2010) 104528.
- [56] S. Takahashi and S. Maekawa, *Spin injection and detection in magnetic nanostructures*, *Phys. Rev. B* **67** (2003) 052409 [[cond-mat/0212317](#)].
- [57] F. Giazotto and F. Taddei, *Superconductors as spin sources for spintronics*, *Phys. Rev. B* **77** (2008) 132501 [[arXiv:0711.0662](#)].
- [58] S. Franco, A. Garcia-Garcia and D. Rodriguez-Gomez, *A general class of holographic superconductors*, *JHEP* **04** (2010) 092 [[arXiv:0906.1214](#)] [[INSPIRE](#)].
- [59] S. Franco, A.M. Garcia-Garcia and D. Rodriguez-Gomez, *A holographic approach to phase transitions*, *Phys. Rev. D* **81** (2010) 041901 [[arXiv:0911.1354](#)] [[INSPIRE](#)].
- [60] F. Aprile, S. Franco, D. Rodriguez-Gomez and J.G. Russo, *Phenomenological models of holographic superconductors and Hall currents*, *JHEP* **05** (2010) 102 [[arXiv:1003.4487](#)] [[INSPIRE](#)].
- [61] N.J. Evans and M. Petrini, *Superfluidity in the AdS/CFT correspondence*, *JHEP* **11** (2001) 043 [[hep-th/0108052](#)] [[INSPIRE](#)].
- [62] F. Denef and S.A. Hartnoll, *Landscape of superconducting membranes*, *Phys. Rev. D* **79** (2009) 126008 [[arXiv:0901.1160](#)] [[INSPIRE](#)].

- [63] J.P. Gauntlett, J. Sonner and T. Wiseman, *Holographic superconductivity in M-theory*, *Phys. Rev. Lett.* **103** (2009) 151601 [[arXiv:0907.3796](#)] [[INSPIRE](#)].
- [64] J.P. Gauntlett, J. Sonner and T. Wiseman, *Quantum criticality and holographic superconductors in M-theory*, *JHEP* **02** (2010) 060 [[arXiv:0912.0512](#)] [[INSPIRE](#)].
- [65] A. Donos, J.P. Gauntlett, N. Kim and O. Varela, *Wrapped M5-branes, consistent truncations and AdS/CMT*, *JHEP* **12** (2010) 003 [[arXiv:1009.3805](#)] [[INSPIRE](#)].
- [66] M. Cvetič et al., *Embedding AdS black holes in ten-dimensions and eleven-dimensions*, *Nucl. Phys.* **B 558** (1999) 96 [[hep-th/9903214](#)] [[INSPIRE](#)].
- [67] L. Romans, *Gauged $N = 4$ supergravities in five-dimensions and their Magnetovac backgrounds*, *Nucl. Phys.* **B 267** (1986) 433 [[INSPIRE](#)].
- [68] S.S. Gubser, C.P. Herzog, S.S. Pufu and T. Tesileanu, *Superconductors from superstrings*, *Phys. Rev. Lett.* **103** (2009) 141601 [[arXiv:0907.3510](#)] [[INSPIRE](#)].
- [69] M. Ammon, J. Erdmenger, M. Kaminski and P. Kerner, *Superconductivity from gauge/gravity duality with flavor*, *Phys. Lett.* **B 680** (2009) 516 [[arXiv:0810.2316](#)] [[INSPIRE](#)].
- [70] M. Ammon, J. Erdmenger, M. Kaminski and P. Kerner, *Flavor superconductivity from gauge/gravity duality*, *JHEP* **10** (2009) 067 [[arXiv:0903.1864](#)] [[INSPIRE](#)].
- [71] F. Bigazzi, R. Casero, A. Cotrone, E. Kiritsis and A. Paredes, *Non-critical holography and four-dimensional CFT's with fundamentals*, *JHEP* **10** (2005) 012 [[hep-th/0505140](#)] [[INSPIRE](#)].
- [72] R. Casero, E. Kiritsis and A. Paredes, *Chiral symmetry breaking as open string tachyon condensation*, *Nucl. Phys.* **B 787** (2007) 98 [[hep-th/0702155](#)] [[INSPIRE](#)].
- [73] S. Sugimoto and K. Takahashi, *QED and string theory*, *JHEP* **04** (2004) 051 [[hep-th/0403247](#)] [[INSPIRE](#)].
- [74] R. Casero, A. Paredes and J. Sonnenschein, *Fundamental matter, meson spectroscopy and non-critical string/gauge duality*, *JHEP* **01** (2006) 127 [[hep-th/0510110](#)] [[INSPIRE](#)].
- [75] G. Bertoldi, F. Bigazzi, A. Cotrone and J.D. Edelstein, *Holography and unquenched quark-gluon plasmas*, *Phys. Rev.* **D 76** (2007) 065007 [[hep-th/0702225](#)] [[INSPIRE](#)].
- [76] A. Sen, *Dirac-Born-Infeld action on the tachyon kink and vortex*, *Phys. Rev.* **D 68** (2003) 066008 [[hep-th/0303057](#)] [[INSPIRE](#)].
- [77] M.R. Garousi, *D-brane \bar{D} -brane effective action and brane interaction in open string channel*, *JHEP* **01** (2005) 029 [[hep-th/0411222](#)] [[INSPIRE](#)].
- [78] M.R. Garousi, *On the effective action of D-brane- \bar{D} -brane system*, *JHEP* **12** (2007) 089 [[arXiv:0710.5469](#)] [[INSPIRE](#)].